Volume 2
Number 10
October 2024
Pages 2719–3154

RSC Sustainability

rsc.li/rscsus

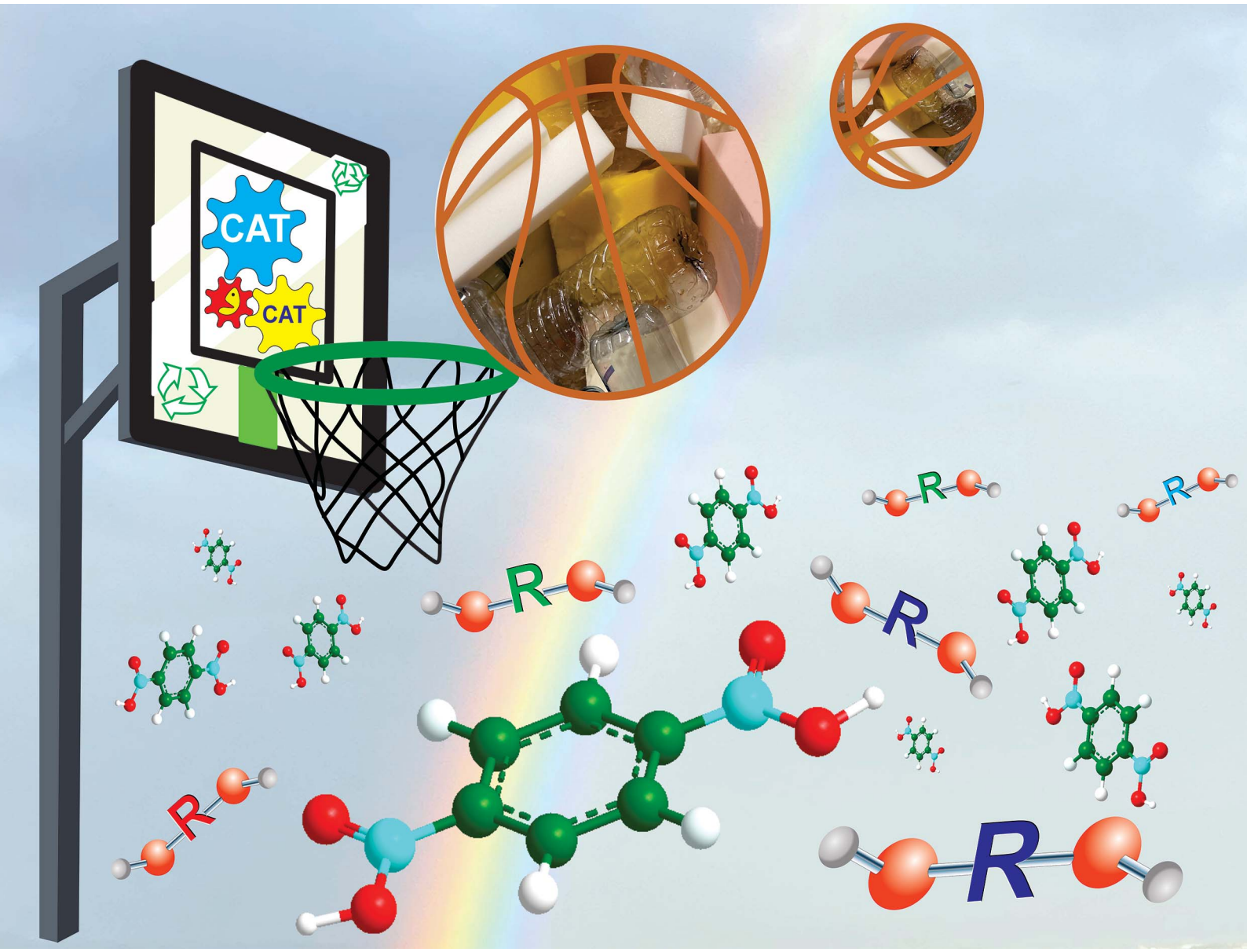

ISSN 2753-8125

ROYAL SOCIETY OF CHEMISTRY

TUTORIAL REVIEW

Francisco G. Cirujano, Belén Altava, Pedro Lozano, Eduardo García Verdugo *et al.*
On the metal- and bio-catalyzed solvolysis of polyesters and polyurethanes wastes

RSC Sustainability

ROYAL SOCIETY OF CHEMISTRY

TUTORIAL REVIEW

View Article Online
View Journal | View Issue

Cite this: *RSC Sustainability*, 2024, **2**, 2781

On the metal- and bio-catalyzed solvolysis of polyesters and polyurethanes wastes

Francisco G. Cirujano, †*[a] Rocio Villa,†[b] Rebeca Salas,[b] Miguel Maireles,[a] Nuria Martín,[a] Belén Altava, *[a] Pedro Lozano *[b] and Eduardo García Verdugo *[a]

Catalysis is a crucial tool to efficiently address the recycling and upgrading of polymeric waste within the context of a circular economy, providing affordable and selective methods for waste valorization in alignment with the principles of green chemistry. Various catalysts, including metals, metal–organic frameworks, and biocatalysts, have been explored for the degradation of chemical poly(ethylene terephthalate) (PET) and polyurethane (PU) waste through processes like hydrolysis or alcoholysis. This critical review specifically focuses on catalytic tools, examining both homogeneous systems (such as metal salts or coordination organometallic complexes) and heterogeneous systems where the catalysts are immobilized on solids, including metal oxides, layered or porous solids, or inorganic–organic coordination polymers as well as biocatalytic counterparts from 2017 to the present. We provide a comparative analysis of the chemo-catalysts researched, evaluating their performance relative to biocatalysts using a SWOT analysis of both technologies to highlight their strengths and limitations in the context of sustainable waste management practices.

Received 11th May 2024
Accepted 4th September 2024

DOI: 10.1039/d4su00233d

rsc.li/rscsus

Sustainability spotlight

Our consumerist society model is placing an unprecedented demand on resources, resulting in a significant increase in residues and waste generation, which creates fundamental doubts about the sustainability of the model. Among all the industrial activities, the plastic industry has become a cornerstone of modern civilization, while plastic wastes constitute one of the most important problems. The enduring nature of these polymers contributes to widespread environmental pollution, with far-reaching effects not only on land and sea but also on human health due to the pervasive issue of microplastic contamination. The depolymerization of plastic materials, followed by reusing the recovered monomeric products in polymer industry, is an urgent necessity. Our work analyzed how catalysis serves as a crucial tool in efficiently tackling the recycling and upgrading of polymeric waste within the framework of a circular economy, providing affordable and selective methods for waste valorization in alignment with the principles of green chemistry. This work emphasizes the importance of the following UN sustainable development goals, related with: Good health and well-being (SDG 3); Clean water and sanitation (SDG 6); Industry, Innovation and Infrastructure (SDG 9); Responsible consumption and production (SDG 12); Climate action (SDG 13); Life below water (SDG 14); and Life on land (SDG 15).

1 Introduction

The polymer industry, which took off around the 1950s, has shown impressive growth from its humble beginnings with an annual consumption of 15 million metric tons to a staggering 390.7 million metric tons by 2021.[1] This industry has become a cornerstone of modern civilization, influencing a broad range of sectors by underpinning crucial products and applications. Polymers are used in everything from packaging materials and medical devices to consumer goods, automotive components, and construction materials.[2,3] Their versatility, durability, and cost-effectiveness have not only revolutionized these industries but also driven innovation and economic growth.[4] Moreover, the polymer industry plays a critical role in addressing modern challenges such as sustainability and environmental impact. It has been instrumental in developing lightweight materials that reduce energy consumption in mobility, packing, and construction, as well as components for renewable energy sources like wind turbines.[5,6]

Despite its success, the polymer industry faces significant environmental and social challenges.[7] According to Plastics Europe (2022), Europe produced 57.2 Mt of plastics in 2021 and generated 29.5 Mt of plastic waste in 2020 and it is estimated that 65% of this plastic waste was landfilled or incinerated and only 35% was sent to recycling.[1,8,9] Moreover, it is predicted that the amount of global plastic waste will increase from 260 to 460 metric tons annually from 2016 to 2030,[10] and that more than

[a]*Department of Inorganic and Organic Chemistry, Universitat Jaume I, Av. Vicent Sos Baynat, s/n, 12006, Castelló de la Plana, Castelló, Spain. E-mail: cirujano@uji.es; altava@uji.es; cepeda@uji.es*

[b]*Departamento de Bioquímica y Biología Molecular B e Inmunología, Facultad de Química, Regional Campus of International Excellence "Campus Mare Nostrum", Universidad de Murcia, 30071 Murcia, Spain. E-mail: plozanor@um.es*

† This authors contributed equally.

500 million metric tons of plastics will be required in 2050.[11] Indeed, the impact of plastics on the environment is huge, as one can estimate, on the one hand, by the millions of metric tons of plastics per year delivered to the oceans, and on the other hand, by the large consumption of global petroleum estimated by 2050 (*ca.* 20%) only for plastics manufacturing. The persistent nature of polymers contributes to widespread environmental pollution, a problem exacerbated in regions with inadequate waste management infrastructures. This has led to significant environmental impact, which is manifested through pollution on both land and sea and the challenge of microplastic contamination. Over 98% of polymers derive from fossil fuels, and prevalent disposal methods like incineration significantly contribute to CO_2 emissions. Additionally, although any biodegradable polymer is often considered greener as it does not generate visible permanent wastes, microbial degradation is a biological oxidation process that yields CO_2 as final product. Thus, regardless of the origin of the starting materials for the production of polymeric materials, the recovery, depolymerisation and reuse of these materials is the most sustainable way to combat waste generation, where CO_2 emission is the most invisible exponent.

The linear economic model of our society, based on the take-make-use-waste should be towards a circular model, where plastic wastes should be considered as chemical feedstocks, achieving the complete recirculation of molecules and materials.[12,13] The Circular Economy Action Plan, introduced in 2015 to push the efforts to improve the circularity in Europe,[14] responds to escalating environmental degradation and health concerns arising from resource inefficiency and emissions,[15] such as the challenging plastic sources.[16] The concept of the circular economy replaces the traditional "dispose" step with a "recycle/reuse" step, emphasizing the reuse of materials instead of the current linear product life cycle management processes.[17,18] For a sustainable circular economy of polymers and plastics, chemistry should favour decoupling from fossil raw material inputs and contribute to achieving zero CO_2 emission by incorporating recycled and biobased feedstock. Only then can we achieve many of the 17 Sustainable Development Goals (SDG) set by the United Nations, 19 such as SDG 3 "Good Health and Well-being", SDG 8 "Decent Work and Economic Growth", SDG 9 "industry, innovation, and infrastructure", SDG 12 "Ensure sustainable consumption and production patterns", and SDG 13 "Climate Action". Developing more efficient and economical catalytic methodologies is crucial for achieving sustainable objectives in polymer recycling. Advanced catalytic recycling techniques facilitate the conversion of waste polymers into valuable raw materials that can be reintegrated into the production cycle. This approach not only minimizes environmental impact but also reduces waste production in a sustainable and cost-effective manner.

1.1 Catalysis as the key enabling tool for plastic recycling

This review explores the development of novel chemical and biochemical transformations aimed at the efficient recovery and recycling of polymer materials to mitigate their impact on the environment.[19–29] Despite the interest of bio-based polymers (able to be degraded by green solvents, supercritical processes and catalysts),[30] special attention will be given to the recycling of polyethylene terephthalate (PET) and polyurethane (PU), as shown in Scheme 1 (top part), which are significant due to their high production volumes and applications ranging from textiles to food and beverage containers.[31–35] For recent literature review on polyester depolymerisation please refer to ref. 29c and 29d. The review will cover different recycling processes, particularly focusing on catalytic chemical recycling techniques, which, though less common, are anticipated to play a significant role in future waste management strategies to provide a detailed understanding of the current challenges and innovations within the polymer recycling industry. The need for integrated approaches that consider environmental impacts, technological advancements, and economic factors in developing sustainable polymer lifecycle management strategies will be emphasized.

From a sustainability perspective, the use of non-toxic and abundant first-row transition metals as catalysts is particularly promising. Thus, the chemocatalytic part of the review will be focused mainly on metal catalysis, and the reader is referred to recent works on other approaches such as organocatalysis.[36–39] Special attention will be paid to the immobilization of these metals within various frameworks, both organic and inorganic, as depicted in Scheme 1 (bottom part). This immobilization results in robust and reusable heterogeneous catalysts that facilitate recycling without significantly contaminating the polymers or monomers. On the other hand, enzymes represent the most active and selective catalysts operating under mild, non-toxic conditions, making them, from a green chemistry point of view, ideal for polymer, *e.g.* polyurethane, solvolysis.[40] However, the high cost and fragility of enzymes as homogeneous biocatalysts have encouraged interest in developing more versatile, stable heterogeneous catalysts that bridge the gap between traditional inorganic metal catalysts and biological catalysts. In this context, the review also includes recent developments in heterogeneous catalysts such as porous metal oxides or metal–organic frameworks to provide a fresh perspective on the interplay between chemical and biological catalysis.

Table 1 summarizes the different catalytic approaches considered in this work, according to the nature of the active site, either discrete active sites (part 2), sites dispersed in extended dense (part 3) or open porous networks (part 4), or biocatalyst (part 5) approaches for the solvolysis of these type of polymers.

2 Discrete metal ions

2.1 Low valence metal catalysts: the special case of Zn(II)-based catalysts

Either rigid and flexible polyurethane (PU) foam was degraded (*via* glycolysis) into polyol (see Scheme 2), with $FeCl_3$ as the most active catalyst precursor (1 wt%) among different 1st-row transition metals such as Zn, Co, Ni and Fe in the form of metal chloride salts.[41] Temperature and reaction time and the type of diol (ethylene glycol (EG) or 1,4-butanediol, being the first more

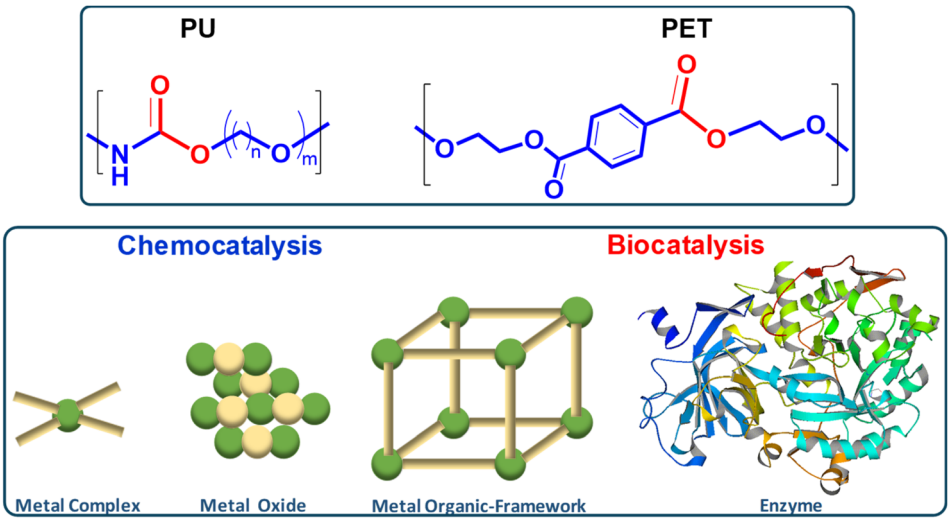

Scheme 1 Similarities and differences between PU and PET condensation polymers reviewed here (top). Discrete metal ions, organometallic complexes, metal oxides and porous metal–organic frameworks as chemocatalysts *vs.* enzyme biocatalysts (bottom).

Table 1 Transition metal catalysts and biocatalysts employed in the degradation of PET and/or PU

Active site	Catalyst	Solid	Porous	Polymer
Zn	$ZnCl_2$	No	No	PU/PET
	$Zn(OAc)_2$	No	No	PU/PET
	ZnO	Yes	Yes	PET
	ZnO/SiO_2	Yes	Yes	PET
	Zn-MOF	Yes	Yes	PET
Fe	$FeCl_3$	No	No	PU
	Fe_2O_3	Yes	No	PET
Sn	SnOctoate	No	No	PU
	Sn/Zn/Al-LDH	Yes	Yes	PU
Ti	$TiOBu_4$	No	No	PU
	TiO_2–SO_4	Yes	No	PET
His, Asp, Ser	Cutinase	No	No	PET
His, Asp, Ser	PETase	No	No	PET
Cu, polypeptide	Laccase	No	No	PU
His, Asp, Ser	Lipase	No	No	PU
His, Asp, Ser	Urethanase	No	No	PU

active towards polyol generation than the second) were optimized due to their effect on the solubility of the metal salts. In general, no reaction was observed at temperatures below 160 °C, having an increase in the recovered polyol when increasing the temperature from 160 to 200 °C. Neither longer reaction times nor temperatures higher than 200 °C allowed the recovery of polyol due to the thermal decomposition of such products.

On the one hand, intermediate trivalent and divalent hard metal cations behaving as Lewis acids were able to degrade rigid PU to more than 90% of polyols. In the case of highly polarizing metal cations, both degradation and re-polymerization processes are favored, thus decreasing the polyol yield. On the other hand, the reactivity of metal chlorides towards rigid PU degradation seems to be related to their corresponding cation charge density and hardness, according to the following order: Fe^{3+} (44% polyol) > Zn^{2+} (23% polyol) > Co^{2+} (44% polyol). In the case of the iron catalyst, the yield increased with the temperature, where the polyol recovery is maximum at 200 °C (see entries 1–3, Table 2). For reaction times larger than 5 h the polyol molecular weight increases because of its re-polymerization.

The authors proposed two pathways of transesterification reactions occurring during the Lewis acid-catalyzed PU degradation. One is based only on the polymer degradation with no polyol release, and another implies the release and recovery of polyol. The last pathway is disfavored in the case of rigid PU foam with a highly cross-linked structure and highly functionalized polyol products. On the contrary, the use of borderline Lewis acids, such as $CoCl_2$ favors the first pathway of molecular weight decrease with a low polyol release and recovery.

Besides the valorization of PU, the authors employed similar catalysts for the degradation of PET into its bis(2-hydroxyethyl terephthalate) (BHET) monomer (see Scheme 2). However, no clear relation between cation and anion could be established,

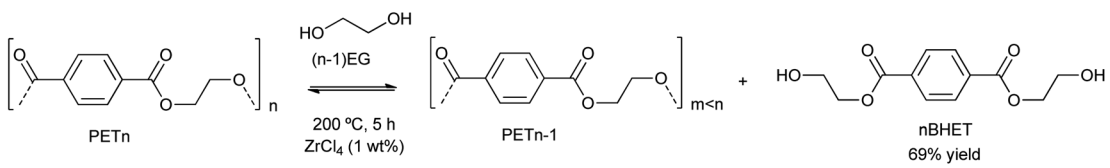

Scheme 2 PET degradation by glycolysis into BHET using metal chlorides, *i.e.* $ZrCl_4$ (1% wt), at 200 °C during 5 h.

Table 2 Comparison between the different (bio)catalysts, conditions and performance for PET and PU degradation

Entry	Catalyst	Substrate	Solvent	Temp. (°C)	Time (h)	Monomer yield	Ref.
1	$FeCl_3$ (1% wt)	PU	EG	200	5	44%	41
2	$ZnCl_2$ (1% wt)	PU	EG	200	5	23%	41
3	$CoCl_2$ (1% wt)	PU	EG	200	5	44%	41
4		PET			5	67%	41
5	$ZrCl_4$ (1% wt)	PET	EG	200	5	69%	41
6	$ZnCl_2$ (70% wt)	PU	H_2O (14 : 1)	140	2	100%	42
7	Zn-salen (8% wt)	PET	EG (27 : 1)	180	2	50%	43
8	Zn-salen (7% wt)	PET	EG (27 : 1)	180	1	60%	44
9	$Zn(OAc)_2$ (1% mol)	PET	EG (7.6 : 1)	196	1	70%	45
10	$Zn(OAc)_2$ (1% wt)	PU	DEG	200	4	48%	46
11	Sn octaoate	PU	EG (15 : 1)	190	4	80%	47
12	ZnO	PET	MeOH	140	2	50%	48
13	ZnO	PET	EG (10 : 1)	210	0.5	100%	49
14	Mo/ZnO (1% wt)	PET	EG (4 : 1)	189	1	90%	50
15[a]	$ZnMn_2O_4$ (1% wt)	PET	EG (12 : 1)	260	1	93%	51
16	ZnO/Al_2O_3 (7.5% wt)	PET	Ethanol (sc)	270	1	90%	52
17	Ni/Al_2O_3 (10% wt)	PET	H_2O sc	270	1	95%	53
18[b]	SO_4–TiO_2 (10% wt)	PET	H_2O (10 : 1) CO_2 sc	160	12	99%	54
19	Fe_2O_3 (2% wt)	PET	EG (13 : 1)	220	0.5	90%	55
20	CeO_2	PET	EG (7 : 1)	196	0.25	90%	56
21	Mg/Zn/Al LDH	PET	EG (10 : 1)	196	3 h	80%	57
22	Zn/Sn/Al LDH (1.3% wt)	PU	DEG (5 : 1)	190	3	66%	58
23	e-MnO_2	PET	EG (55 : 1)	200	0.5	100%	59
24	ZnO/SBA-15 (5%)	PET	EG (4 : 1)	200	1	90%	60
25	MAF-6	PET	EG (6 : 1)	180	4	82%	61
26	Leaf-branch compost cutinase (LCC)	PET	0.1 M potassium phosphate, pH 8	72	10	90%	62*a*
27	PETase	PET	50 mM potassium phosphate buffer, pH 7.2	30	1	78%	63
28	Ca^{2+}(1 M)/LCCICCG	PET	50 mM Tris–HCl buffer, pH 8	80	12	84%	64
29	NusA-*Is*PETase^{Mut}	PET	50 mM Gly-NaOH buffer, pH 9	30	14 days	19.6% (weight loss)	65*a*
30	*S238Y-Is*PETase^{Mut}	PET	50 mM Gly-NaOH buffer, pH 9.4	30	72	~3% (crystallinity loss)	65*b*
31	*RITK-cutinase*^{Mut}	PET	100 mM potassium phosphate buffer, pH 8	72	24	90%	66
32[c]	H_2O	PET	H_2O	250	1.5	85%	67
33	*Humicola insolens* cutinase		0.1 M Tris–HCl buffer, pH 7	50	24	>99%	
34	*Trametes versicolor* laccase	PU	0.1 M sodium acetate buffer, pH 4.5	37	18 days	17.2% (weight loss)	68
35	*Humicola insolens* cutinase	PU	0.1 M potassium phosphate buffer, pH 8	50	168	42% (weight loss)	69
36	Tfcut2 (cutinase)	Dispersed PU	0.3 M potassium phosphate buffer, pH 8	70	200	0.026 s^{-1}	70
37	LCC (cutinase)	Solid PU solid	0.1 M potassium phosphate buffer, pH 8			5%	
38	*Candida rugosa* lipase	PU	0.1 M potassium phosphate buffer, pH 7	35	1	0.12 mg product per L per min	71
39	Tin(II)-2-ethylhexanoate	PU	DEG	200	2	99%	72
40	UMG-SP-2 (engineered urethanase)		0.1 M potassium phosphate buffer, pH 7.5	30	48	>99%	

[a] 5 bar. [b] 150 bar. [c] 40 bar.

although the interaction of the metal cation with polyester is key, and therefore a combination of cation hardness, charge density and anion softness will control the catalyst-carbonyl group interaction, promoting its degradation. Indeed, an induction period at the beginning of PET degradation suggested this metal-carbonyl interaction, after which the ethylene glycol attacks the Lewis acid-activated ester groups, resulting in the solubilization/degradation of PET in the alcohol, medium. The highest yields of (BHET) were obtained with $ZrCl_4$ (69%) and $CoCl_2 \cdot 6H_2O$ (67%) catalysts at 200 °C, while no yield was observed for the blank reaction (see entries 4–5, Table 2).

Wang *et al.* proposed the efficient PU degradation, *via* selective cleavage of C–O/N bonds by coordinatively unsaturated Zn(II) species formed in highly concentrated 70% $ZnCl_2$ aqueous solutions.[42] The electrophilic Zn(II) cations behave as Lewis acid for the activation (*via* coordination) of the oxygen and nitrogen heteroatoms present in the functional groups of PU substrate. This resulted in the eventual cleavage of C=O

urethane linkages and C–N bonds by the $ZnCl_2$, used in a weight excess of 14 : 1 with respect to the PU, at 140 °C for 2 h (see entry 6, Table 2). By FTIR and NMR, 2,4-diaminotoluene (DAT), polytetramethylene ether glycol (PTMEG) and 3,3′-dichloro-4,4′-diaminodiphenylmethane (MOCA) were detected as the products of PU degradation (see Scheme 3). However, the C–C and C–O–C bonds were not altered by the Zn(II) of ether linkages as the framework structure remained intact in the degradation process. The mechanism of selective cleavage of C–O and C–N bonds of urethane resulted in the production of carbamic acid (which produced CO and the corresponding amine) and alcohol (PTMEG), which was no further cleavage at the C–O ether bonds.

A similar 70 wt% $ZnCl_2$ aqueous solution was employed for the selective solvolysis of a polyester/polyurethane-coated textile composed of PET fabrics coated with bio-based PU, simplifying the separation of the coating from the fabric for further recycling.[73] Suprastoichiometric amounts of $ZnCl_2$ (17.5 times more weight) were employed with respect to the PU-coated polyester under aqueous conditions at 140 °C for 2 h. In this case, the Zn(II) Lewis acid sites are in a cheaper medium with respect to deep eutectic solvents (DES) and ionic liquids (IL). FTIR analysis of the products at the liquid fraction indicated the formation of primary amines and isocyanurates, as well as the polyester polyol (some of them oxidized to aldehydes by the Zn sites). Interestingly, the polyester was not degraded under the conditions employed.

Different salen-type zinc complexes, prepared from amine-aldehyde condensations (see Scheme 4a), were reported for the methanolysis of polylactic acid (PLA) at 80 °C and glycolysis of PET from carbonated drinks bottles to form bis(2-hydroxyethyl) terephthalate (BHET).[43] Around 50% yield to colorless (after recrystallization) BHET was obtained after 2 h, working at 180 °C in the presence of 8 wt% loading and 27 equivalents of ethylene glycol (EG) with respect to ester linkages (see entry 7, Table 2).

Homoleptic zinc complexes linked by monoanionic phenoxy-imine pyridine moieties were active catalysts in the alcoholysis of PLA and glycolysis of commercial poly(ethylene terephthalate) samples.[44] The Zn active site is located in a plane with two (almost perpendicular) bidentate ligands. The salen group chelates the metal while one pendant pyridine points in the other direction to the metal center (see Scheme 4b). The PET sample was contacted with 27.8 equivalents of ethylene glycol in the presence of 0.013 equivalents of Zn (both with respect to the

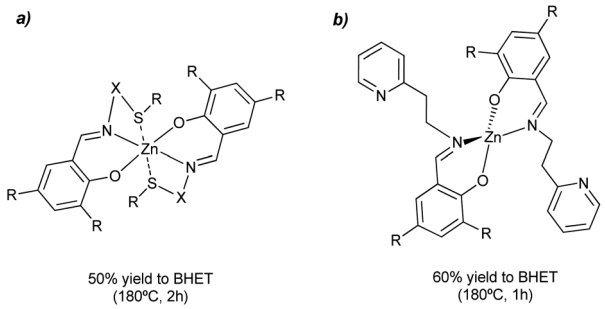

Scheme 4 Salen-Zn catalyst (8 wt%), without (a) or with (b) pendant pyridine groups, for the glycolysis of PET into BHET at 180 °C for 1–2 h.

ester functionalities) at 180 °C for 1 h. Under such conditions, up to 95% conversion and 60% yield of BHET was obtained (see entry 8, Table 2). Similar amounts of ZnO required 4 h to convert 72% of the PET, obtaining only 20% yield of BHET. The reported catalyst also outperformed the benchmark zinc acetate, which produced 40% yield of BHET after 4 h while using seven times more catalyst. The zinc sites should work as Lewis acid catalysts that activate the carbonyl group while the pyridine groups might abstract the proton from the alcohol solvent. However, more investigation is needed to understand the catalyst's reaction mechanism and stability under *operando* conditions. Other authors employed zinc acetate $Zn(OAc)_2$ (1 mol% with respect to PET) as a catalyst for PET granules wastes degradation in EG.[45] After 1 h, a BHET yield of 70% was obtained at 196 °C, using an excess of EG : PET molar ratios of 3.8 (see entry 9, Table 2). In contrast, no appreciable yield was detected until 6 h for the blank reaction at 196 °C, even with an EG : PET ratio of 7.6. Alternative catalysts to transition metals, such sodium carbonate, were tested as a depolymerization catalyst, given the lower price and toxicity with respect to Zn. However, higher PET : catalyst molar ratios were needed to achieve similar BHET yields as those obtained with Zn (*i.e.* PET : Na = 245 *vs.* PET : Zn = 380). Other sodium salts such as sodium sulfate give poor product yields. This was attributed to the lower solubility with respect to the carbonate. Regarding the mechanism, the formation of Na/Zn-carbonyl intermediates during the transesterification reaction process were proposed. In fact, the metal–oxygen bonds between the catalytic active metal site and the functional groups at the PET substrate are shorter for Zn (2.26 Å) than for Na (2.41 Å). Therefore, a better activation of the ester group by the Zn(II) results in a faster nucleophilic attack by the EG.

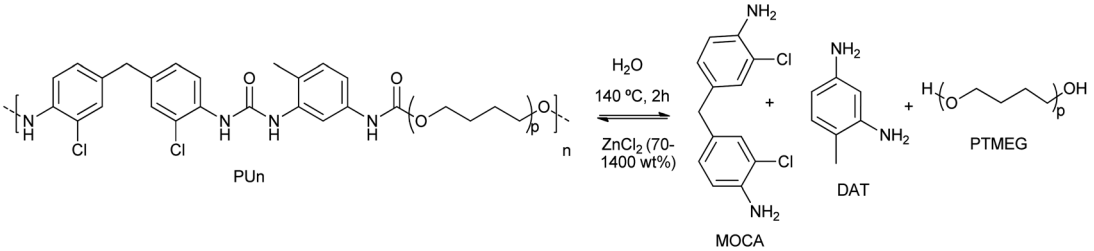

Scheme 3 Controllable degradation of PU using $ZnCl_2$ (70–1400 wt%) as a supra-stoichiometric reagent at 140 °C for 2 h.

Grounded polyurethane foam wastes at 200 °C in diethylene glycol (DEG) was depolymerized (transesterified) in the presence of zinc acetate (1 wt%) as a catalyst (Scheme 5a).[46] This zinc-based homogeneous catalyst was more active (48% decrease of the urethane bond area) than organic amine catalysts (see entry 10, Table 2), such as diethylamine (17% decrease of the urethane bond area) or methylamine (25% decrease of the urethane bond area), as authors observed by FTIR. The zinc acetate was also more active than inorganic bases, such as barium or potassium acetates, achieving less than 25% decrease in the urethane bond area. Even the reported tin alkoxide catalyst exhibited lower activity in the PU depolymerization (less than 15% decrease in the urethane bond area). Thus, the divalent Zn ions were key in the activation of the urethane carbonyl group, promoting the nucleophilic attack by the oxygen of the low-weight glycols (see Scheme 5a). On the contrary, the reaction pathway occurring with the tin-based catalysts is different. This is because the alcohol first adds to the tin complex forming an alkoxide intermediate, see for instance their application in split-phase glycolysis.[74–77] Indeed, the formation of the active species in the case of the zinc catalyst is ten times higher than the tin complexes (see Scheme 5b).

2.2 High valence metal catalysts: tin(IV) and titanium(IV)-based systems

Octoate salts of alkaline or transition metal catalysts (such as Li, Na, K, Sr, Co, Ni, Zn and Sn) were reported as active catalysts for the glycolysis of polyurethane.[47,78] On the one hand, scrap foams with a size of 5–25 mm and a composition of polyether polyol poly(propylene oxide-*block*-ethylene oxide) and toluene diisocyanate (TDI) were employed as substrate. On the other hand, a 15 : 1 mass ratio of ethylene glycol (EG) with respect to the scrap PU foam and a metal catalyst concentration of 60 mM were reported.[47] All catalysts completely degrade the polyurethane chain at 190 °C, as determined by the disappearance of the oligourethanes (see entry 11, Table 2). However, different glycolysis rates were obtained depending on the metal. The best performance catalysts were the Li and Sn octoate salts. The high degradation rate and polyol recovery were attributed to the hard Lewis acid nature of the metal cation.[47] Indeed, the interaction of the metal with the hard Lewis base oxygen atom from EG, favors the formation of the metal alkoxide. Note that this intermediate has a non-coordinated hydroxyl group at the glycol that subsequently acts as a nucleophile towards the carbonyl carbon of the urethane group. Besides such first rate-determining step, the transesterification reaction mechanism involves: (i) the formation of a metal alkoxylate, (ii) coordination–insertion of the alkoxide into the urethane group and (iii) transfer from recovered polyol to glycol (see Scheme 6).

In the case of strontium, which was classified as a soft Lewis acid, the PU degradation rate was slower. For Co, Sn and Zn octoate salts the degradation rates were higher than in the case of Ni salts. Thus, there should be some additional stabilization factor of the Sn-complexation (*via* coordination-insertion) to the urethane carbonyl group, as well as the not-too-strong (basic alkaline cations)/not-too-weak metal alkoxide bonding resulting from the metal octoate and EG first reaction step. Interestingly, there is no need to separate the stannous octoate from the obtained polyol phase since this same catalyst is employed in PU foaming from the recovered polyol, so no additional purification steps are required when aiming at this application.[47] The higher activity of the Zn salt is in line with the above-mentioned high-performance zinc catalysts (zinc acetate and zinc chloride) for both PET and PU degradation, which confirms the similarity between both transesterification reactions.[78]

Other authors employed titanium(IV) tetrabutoxide for the dissolution of rigid PU foams at 180 °C in dipropylene glycol (DPG).[79] Although less active than traditional inorganic Brønsted bases, the titanium catalyst requires less time (45 min) than stannous octoate (143 min) for the PU glycolysis

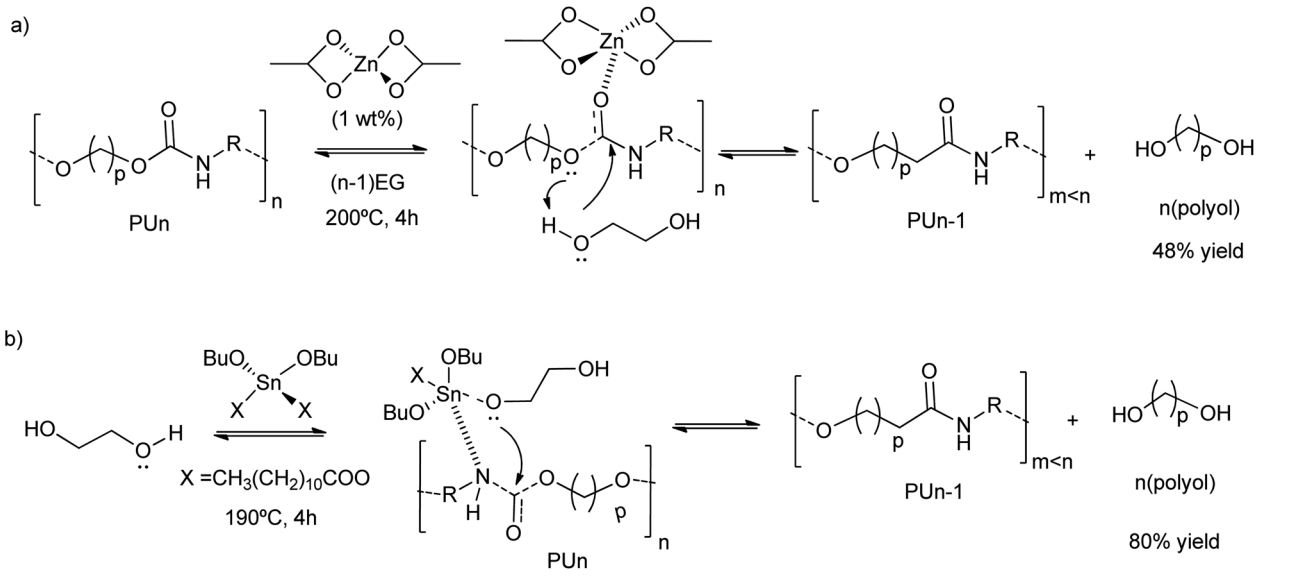

Scheme 5 Proposed mechanisms for PU degradation using $Zn(OAc)_2$ (a) or $Sn(OBu)_2X_2$ (b) as a catalyst at 190–200 °C for 4 h.

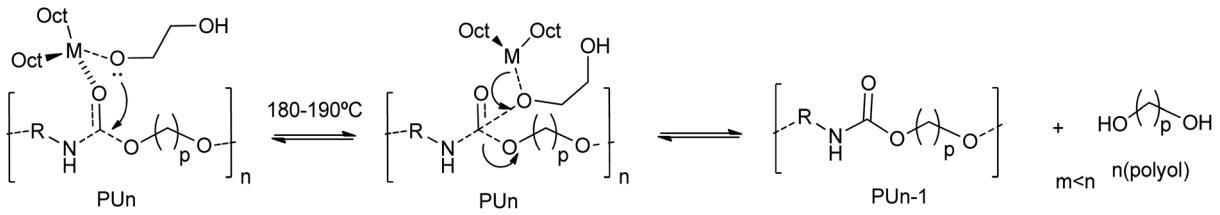

Scheme 6 Proposed mechanisms for PU degradation at 180–190 °C using octoate salts of metals (M = Li, Na, K, Sr, Co, Ni, Zn) as a catalyst.

(0.0036 mol cat./DPG 100 g). This strategy allowed the formation of titanium isopropoxide-derived titanium nanodiol catalysts, consisting of a homogenized nanoscale titanium core coated with an alcohol shell.[80] This provided a more active catalyst, concerning traditional alkali metal-based catalysts, for the glycolysis of waste polyurethane (PU) pipeline foams. A combination of KOH and the titanium catalyst, even in amounts of only 0.05 wt%, decreased the regenerated polyether polyols viscosity by 10% (Scheme 7). However, little information was provided about PU conversion and reaction mechanisms for the sole titanium catalyst.

Finally, we will highlight an example of polyurethane synthesis from PET-based polyols. Three consecutive catalytic steps were carried out to combine the PET degradation and with the PU synthesis from the polyol building blocks obtained. The first step consisted of the glycolysis reaction of PET at high temperatures (230–300 °C) using titanium isopropoxide as catalyst (0.5 wt%).

Crude glycerol was added to the glycolyzed PET oligomeric mixture. The final polyol mixture obtained showed less hydroxyl number and was used as a monomeric mixture for the synthesis of polyurethanes with different physical and chemical properties (*i.e.* density, compressive strength, *etc.*).[81] However, the use of extreme reaction conditions as well as non-selective catalysts generates uncontrolled reactions and side products.

3 Dense metal oxide architectures

3.1 Low valence metal oxides: the special case of ZnO-based catalysts

ZnO nanoparticles were obtained either from the methanolysis or glycolysis of zinc acetate in a solution of KOH in methanol or ethylene glycol, respectively.[48] Methacryloxy and/or amino alkoxysilanes were also employed in the basic alcohol media, probably modulating nanoparticle growth. The colloidal dispersion of ultra-small ZnO nanoparticles (*ca.* 4 nm) has been employed as a pseudo-homogeneous catalyst (see Scheme 8a). PET methanolysis and glycolysis into dimethylterephthalate (DMT) and bis(2-hydroxyethyl terephthalate) or BHET, respectively, were successfully achieved by such catalyst. The adequate dispersion of the nanoparticles in methanol avoids their aggregation of (<20 nm) favoring their accessibility and diffusion of the PET substrate. Using an alcohol : PET weight ratio of six, a 97% yield to DMT was obtained in less than half an hour. When the temperature was decreased to 140 °C, a 50% yield of DMT was obtained after just 2 h (see entry 12, Table 2). This corresponds to 553 and 117 $g_{PET}\ h^{-1}\ g_{ZnO}{}^{-1}$, for the methanolysis and glycolysis, respectively. On the other hand, the glycolysis of PET was 4 times slower compared to the methanolysis. The methanolysis occurred from the outside to the inside of the PET, decreasing the particle size of the polymer and increasing its porosity. Key to the mechanism was the activation of the carbonyl bond by the Zn atoms of the nanoparticles, acting as Lewis acid catalysts. Simultaneously, the adjacent oxygen atoms assisted in the deprotonation of the alcohol solvent, which eventually broke the ester linkages generating methyl ester oligomers (see Scheme 8).

A solution containing polyvinyl pyrrolidone (PVP), zinc acetate and sodium hydroxide in ethanol or pentanol/ethanol resulted in ZnO nanorods and ZnO nanoplates, respectively.[49] Using an EG : PET molar ratio of 10 at 210 °C, a 100% conversion was achieved in half an hour (see entry 13, Table 2). Most importantly, the heterogeneous ZnO could be separated by filtration and recycled in two additional reaction cycles with similar performance as the as-prepared material. At left part of Scheme 9 the authors proposed that the smaller the size of the ZnO nanoparticle (for the same morphology), the higher the catalytic activity (>20% increase in conversion and yield). This was attributed to the large (macromolecular) size of the substrate, favoring its mass transfer to the Zn Lewis acid sites at the small nanoparticles.

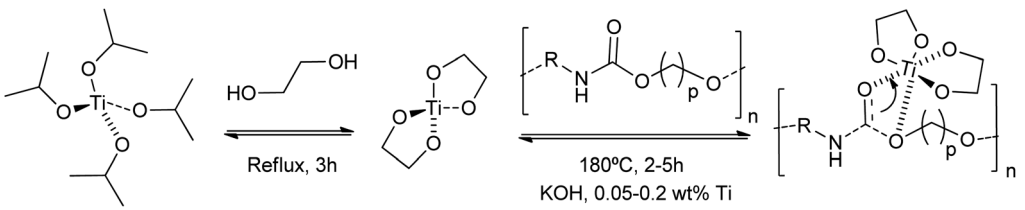

Scheme 7 Proposed mechanisms for hard PU degradation at 180 °C for 2–5 h using KOH and 0.05–0.2 wt% Ti-glycol nanocatalysts prepared from titanium isopropoxide and ethyleneglycol.

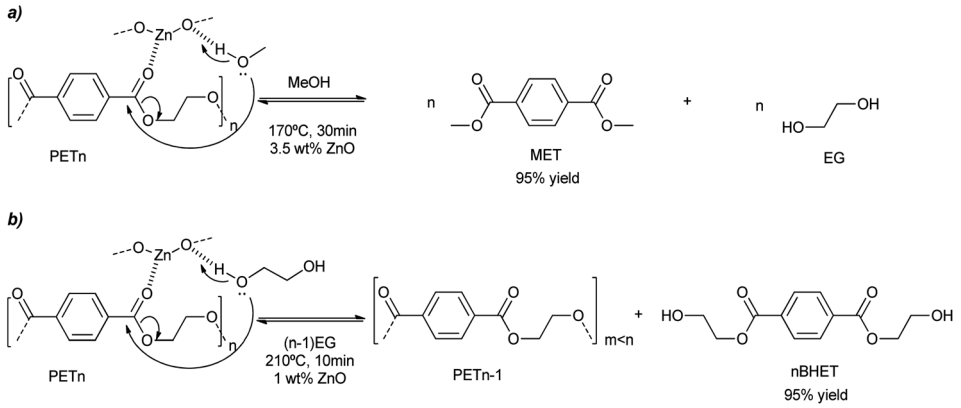

Scheme 8 PET degradation mechanism by methanolysis (a) or glycolysis (b) into MET or BHET, respectively, promoted by ZnO nanoparticles (1 wt%) at 210 °C for 10 min.

The authors also point to the important effect of the oxygen atoms adjacent to the Zn sites in withdrawing electron charge from the zinc Lewis acid sites. They also promote hydrogen bonds with ethylene glycol, thus, acting as Lewis base sites with the hydrogen atom from the hydroxyl group of the EG nucleophile (see Scheme 8b). Moreover, (001) facets are more exposed in the case of hexagonal ZnO samples (prisms, disks, and platelets), even for relatively larger crystal size (>250 nm), enhancing its catalytic activity for PET glycolysis (see right part of Scheme 9). Furthermore, the authors point out that microwave heating is superior to conventional heating for PET glycolysis, achieving excellent conversion and yields in short reaction times.[49]

ZnO nanosheets and nanorods were prepared from thermal decomposition of a zinc/asparagine precipitate in the presence or absence of Mo/Co-sources.[50] Only 1 wt% of catalyst was employed for the glycolysis of PET (4 : 1 EG : PET mass ratio) at 180 °C for 1 h. Less than 60% conversion and BHET monomer yield were obtained with pristine ZnO nanoparticles. On the contrary, those with Co or Mo atoms in its lattice led to

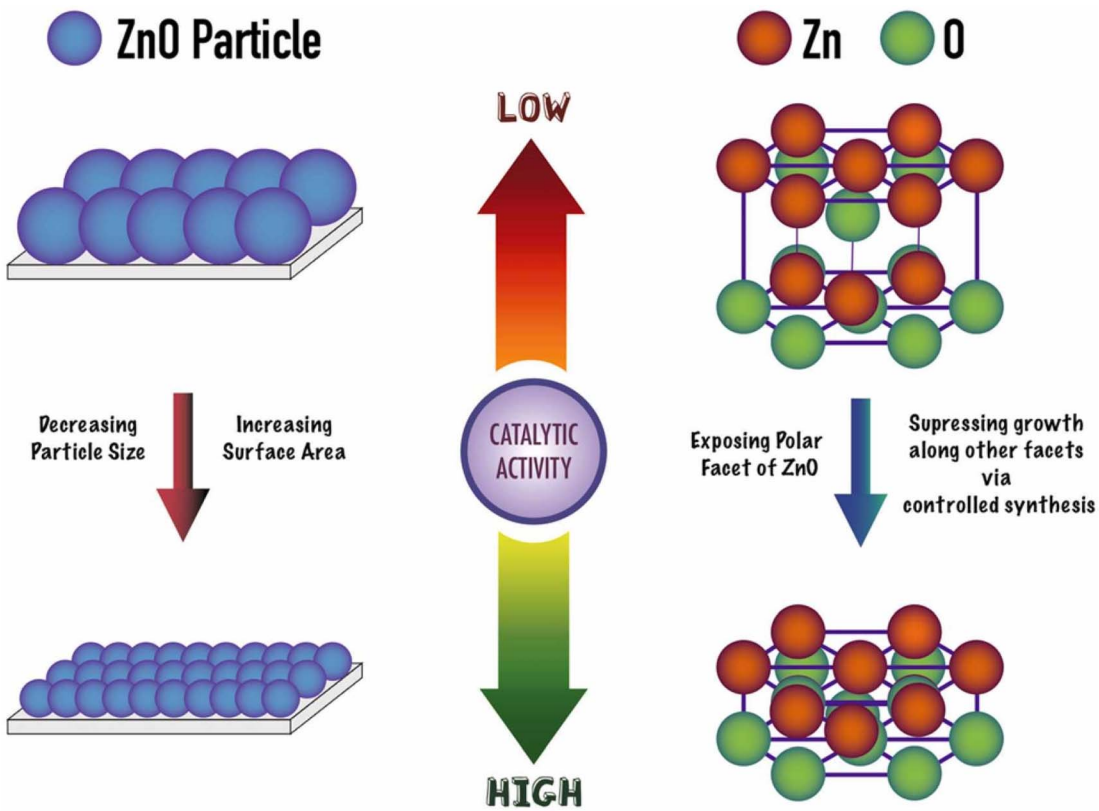

Scheme 9 Geometric effects on PET glycolysis activity of ZnO nanoparticles. Reproduced with permission of ref. 49. Copyright (2023) Elsevier.

quantitative conversions and BHET yields (>90%, see entry 14, Table 2).

The presence of Mo favors the formation of ZnO (100) surfaces with abundance of Zn defects and O vacancies. Atomically dispersed Mo–O and Co–O sites at oxygen bridge bonds of ZnO nanosheets drive the formation of electronically tunable dual Zn–O, Mo–Zn and Co–Zn active sites. XPS analysis of the Mo-doped ZnO suggests electron density migration from Mo to Zn *via* the O-bridges. Both oxygen vacancies and zinc defects are beneficial for the activation of: (i) the alcohol group (deprotonation) of EG, and (ii) the ester group (carbonylic oxygen) of the PET substrate (see blank inserts in Scheme 10).

The doping of Mo leads to the enhancement of the covalence of the Zn–O bond, which is proposed to lead to electron transfers and the formation of reactive oxygen species at the surface. This species interacts with the OH groups from the EG to produce adsorbed deprotonated EG (*OCH_2CH_2OH). Therefore, the catalytic synergies of the dual Zn^{2+}–O^{2-} and Mo^{2+}–O^{2-} pairs eventually promote the C–O bond breaking in the PET structure. They also improve the yield of the BHET monomer after subsequent attacks on the ester bonds of PET (Scheme 9b and blank inserts in Scheme 10).

The Mo/ZnO catalyst could be reused in 3 cycles, with only a minor decrease in performance during the first two cycles, which became stronger deactivation in subsequent cycles. However, the catalyst could be regenerated by calcining at 500 °C in air and then at 350 °C under hydrogen. This regenerated the oxygen vacancies and thus maintains its catalytic activity after three additional cycles.[50] Ni-doped MgO exhibited similar Ni^{2+}–O^{2-} acid–base pairs and catalytic behavior, being able to decompose PET *via* glycolysis at 185 °C for 50 min. A 90% yield of BHET monomer was obtained even after 6 reaction cycles, indicating the stable catalytic activity of the composite metal oxide.[82]

A catalyst with a structure of zinc manganite $ZnMn_2O_4$ tetragonal spinel was employed for PET hydrolysis. The Zn-based spinels contain tetrahedrally coordinated Zn ions and octahedrally coordinated Mn ions at the crystal lattice. Quite harsh reaction conditions were employed (260 °C, 5 bars, 1 h) to quantitatively decompose PET into its BHET monomer. Indeed, 12 equivalents of ethylene glycol and 1 wt% catalyst were employed, both with respect to PET.[51] The 93% yield of BHET obtained with $ZnMn_2O_4$ (see entry 15, Table 2), decreases to 89% and 81% in the case of tetragonal $CoMn_2O_4$ and cubic $ZnCo_2O_4$ spinels. This was attributed to a lower amount of acid sites and BET areas of the Co-containing catalysts. Based on that the authors proposed that the combination of Zn^{2+} and Mn^{3+} cations in the tetragonal $ZnMn_2O_4$ spinel possesses a better capability for activation and breaking the C=O bonds at the acid sites (Scheme 11). This allows the PET polymer to decompose into oligomers and then into monomers during its degradation pathway. Unfortunately, no additional cycles with the spent catalyst were reported to check its stability.

Similar harsh conditions (above the melting point of PET) were employed for the ethanolysis of this condensation polymer when using ZnO (7.5 wt%) on acidic gamma alumina.[52] With a catalyst loading of 5 wt% with respect to PET, >90% yield to diethylterephthalate (DET) was obtained after 1 h in supercritical ethanol at 270 °C (Scheme 12a and entry 16, Table 2). Some activity loss was observed since the 5th recycle decreased the

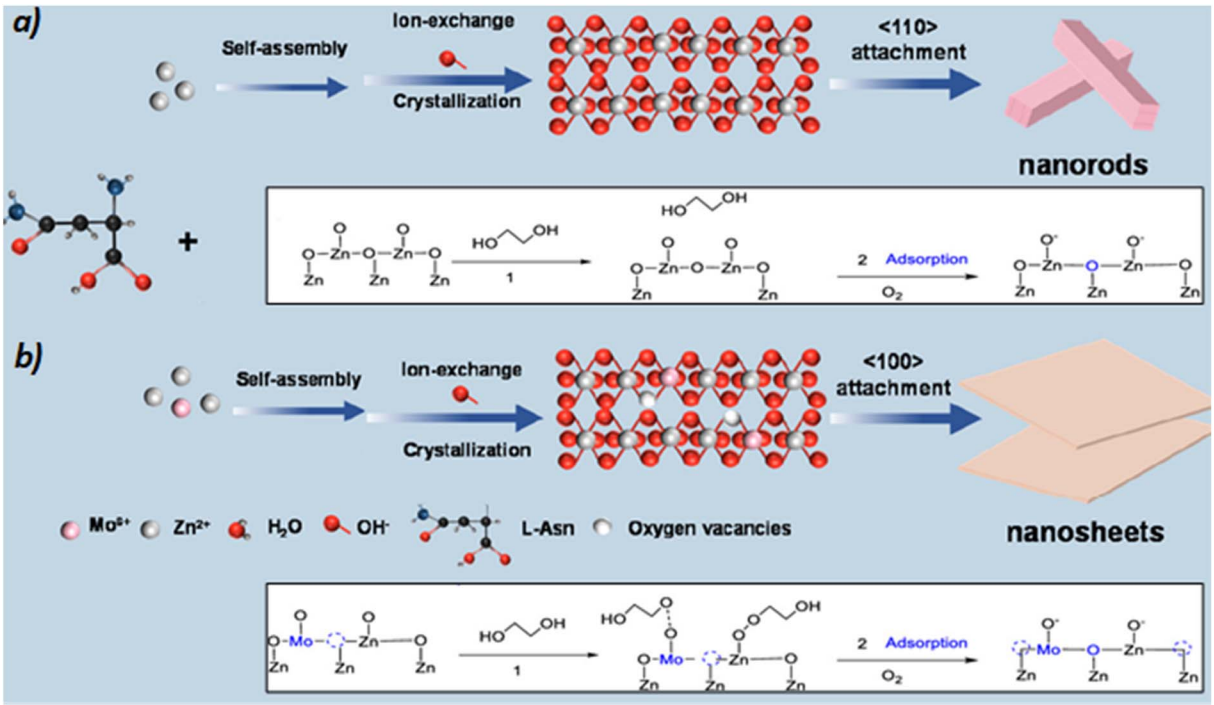

Scheme 10 Synthesis of ZnO nanorods and Co/ZnO (a) or Mo/ZnO nanosheets (b), together with the tentative glycolysis pathway in each of them. Adapted with permission of ref. 50. Copyright (2022) American Chemical Society.

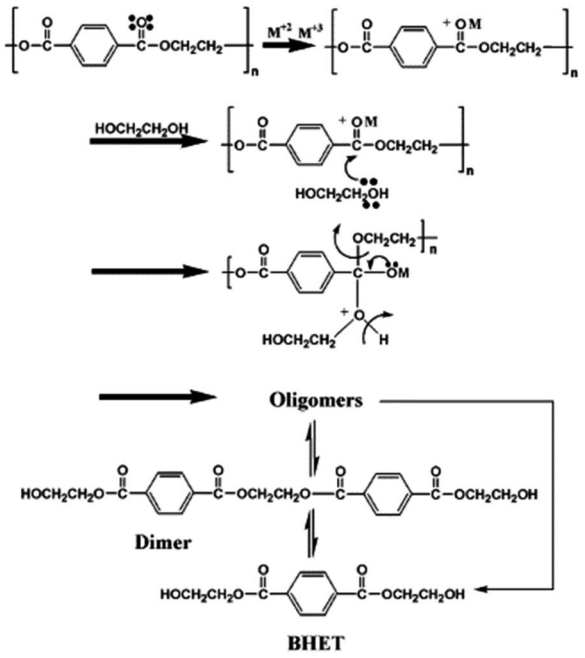

Scheme 11 PET glycolysis mechanism over double metal oxide catalysts. Adapted with permission of ref. 51. Copyright (2013) Elsevier.

DET yield to 75% due to the loss of the ZnO component. Aiming at hydrolysis of PET, nickel was impregnated on alumina, with loadings of 10–15 wt%. Using supercritical water at 260–270 °C, >95% yield of terephthalic acid was obtained after 1 h with the calcined/hydrogenated catalyst (see Scheme 12b and entry 17, Table 2).[53] However, the yield decreases to less than 80% after the third cycle. This was probably due to the formation of carbon deposits at the porous support that blocks the metal active sites. Thus, regeneration of the catalyst (calcining at 600 °C to burn the carbon deposits) is necessary, increasing the activity and product yields to 90%.

The interface growth of ZnO and CuO mix metal nanoparticles was reported by bicarbonate assisted co-precipitation of their nitrate precursors.[83] The calcination of the oxides allowed for the Cu^{2+} substitution by Zn^{2+} in the malachite phase ($Cu_2(OH)_2CO_3$), and Zn^{2+} substitution by Cu^{2+} in the hydrozincite phase ($Zn_5(OH)_6(CO_3)_2$). This fact allowed the tuning of the catalytic activity of the mix-metal oxide for the decomposition of dimethylhexane-1,6-dicarbamate (HDC in Scheme 13a) at 175 °C. Using a ten times mass excess of polyethylene glycol dimethyl ether as solvent, a 70% conversion (after 1 h) of HDC into hexane-1,6-diisocyanate (HDI in Scheme 13a) was obtained. While low amounts of Zn increase the activity of the material, high Cu/Zn ratios decrease both the surface area and catalytic activity. On the other hand, nano-sized Cu_2O prepared by hydrolysis/calcination (under an inert atmosphere) steps was an active catalyst for the obtention of methylene di(phenylisocyanate) (MDI). This occurs due to the degradation of methylenediphenyl di(phenylcarbamate) (MDPC) under solvent-free conditions and 210 °C (see Scheme 13b).[84] A conversion of 64% based on the MDPC substrate was obtained, with a 48% selectivity to MDI. In comparison, ZnO promoted only a 50% MDPC conversion and 40% selectivity.

3.2 High valence metal oxide catalysts: Fe(III), Sb(III), Ce(IV) and Ti(IV) oxide-based systems

Sulfated titanium dioxide SO_4^{2-}/TiO_2 was prepared by precipitation of $Ti(OH)_4$ and further H_2SO_4 treatment and calcination.[54] The solid catalyst was employed in the degradation, *via* hydrolysis, of PET under supercritical CO_2 at 160 °C and 15 MPa during 12 h, obtaining 99% yield to terephthalic acid (see entry 18, Table 2). The solid catalyst promoted the formation of Brønsted acid sites that were able to protonate the water solvent. Such water and hydronium ions degrade the PET from the surface and the inside (bulk) promoting the swelling and hydrolysis of the PET. The same authors promoted the same catalytic process but using titania with surface WOx species as

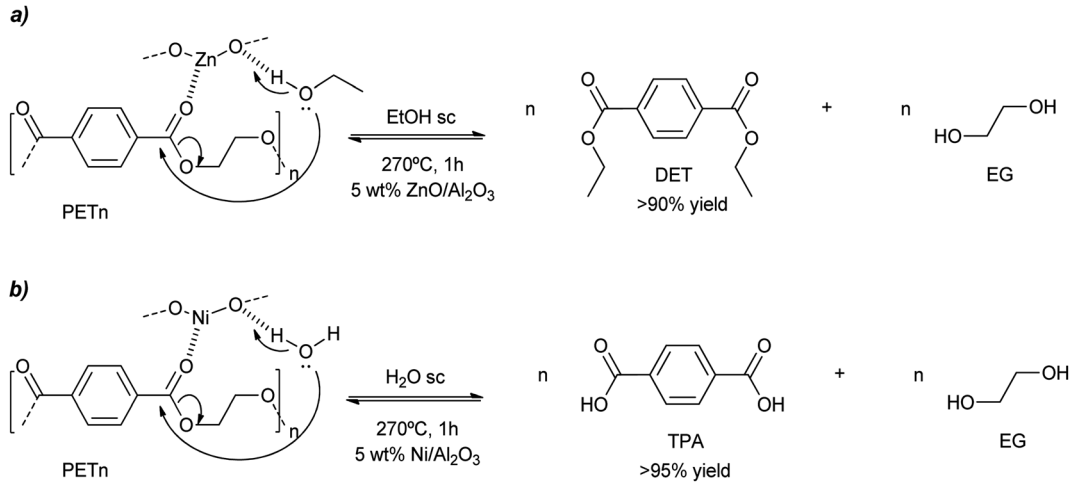

Scheme 12 PET degradation mechanism by ethanolysis (a) or hydrolysis (b) into MET or BHET, respectively, promoted by ZnO (a) or Ni (b) doped alumina (5 wt%) at 270 °C for 1 h under supercritical ethanol (a) or water (b).

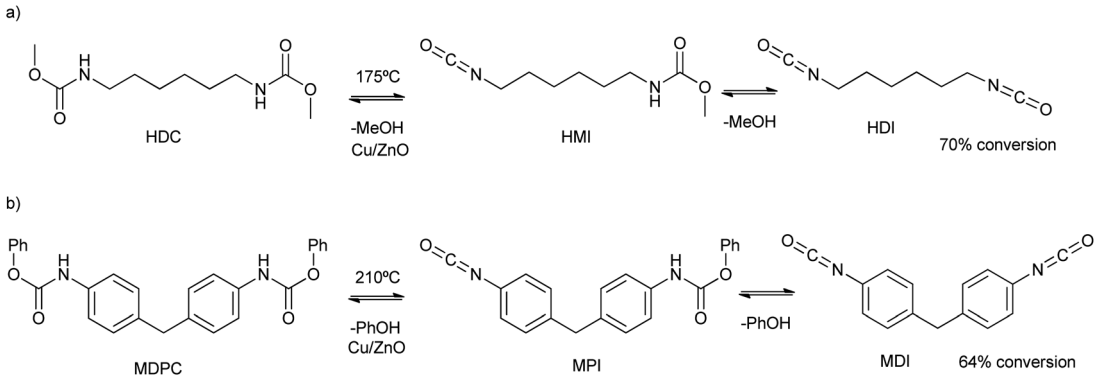

Scheme 13 (a) HDC and HMI degradation mechanism into HDI and methanol at 175 °C; (b) MDPC and MPI degradation mechanism into MDI and phenol at 210 °C.

acid sites.[85] The catalyst preparation, in this case, was hydrothermal and instead of using base-assisted precipitation, a surfactant (CTMABr) was employed. In particular, the number of polytungstate species increases in line with the number of Brønsted sites, which were active in the PET hydrolysis. For that, a PET/catalyst/H_2O mass ratio of 1 : 0.1 : 10 at 160 °C and 15 MPa was employed during 15 h under supercritical CO_2.

Antimony oxide demonstrated a better performance than its antimony acetate precursor in the PET degradation by glycolysis with ethylene glycol (with an EG : PET weight ratio of 5).[86] The yield of BHET, using 0.5 wt% of the catalyst, under 200 °C and 2 bar was 98% after 1 h, while only 64% yield was produced with antimony(III) acetate (see Scheme 14). In the case of the reaction in the absence of any catalyst, only 11% yield of BHET was obtained. However, zinc acetate is still a competitive catalyst with respect to Sb_2O_3, both having a similar performance for PET glycolysis. It is worth mentioning that the monomer containing the antimony catalyst can be employed for further polymerization into PET provided the EG excess is removed by evaporation under vacuum.

Highly dispersed, ultra-small iron oxide nanoparticles (<10 nm) were prepared from the precipitation of iron chloride in a sodium citrate/ammonia medium, resulting in a Fe_3O_4 nanodispersion in EG with a 5 wt% solid content.[55] The citrate adsorbed on the nanoparticle avoids both the aggregation and oxidation of the nanoparticles, which exhibited Brønsted and Lewis acid sites, and more importantly, BET surface areas >100 $m^2\ g^{-1}$. Using a Fe_3O_4/PET = 2% and an EG/PET = 13, more than 90% yield to BHET was obtained at 210 °C for 30 min (see entry 19, Table 2). The yield was maintained even after three cycles and the iron oxide nanoparticles were magnetically separated and reused after washing (ethanol and water) and redispersing in EG.

Ultra-small (*ca.* 3 nm) and highly defective CeO_2 nanoparticles combined significant BET surface areas (>100 $m^2\ g^{-1}$), excellent dispersibility, and a high density of oxygen defects.[56] This resulted in efficient PET depolymerization at 196 °C, using an EG : PET weight ratio of 7. The reaction is completed after 0.25 h, obtaining a 99% conversion of PET and a 90% yield of the monomer yield of 90% (see entry 20, Table 2). The small CeO_2 nanoparticles, containing Ce^{3+} ions that promote lattice strain, eventually contain oxygen defects. Those are key active sites in the cleaving of the ester bonds from the PET substrate, leading to oligomers and MHET and BHET through a dynamic equilibrium (see Scheme 15).

4 Open 2D/3D metal-containing architectures

4.1 Layered 2D frameworks

Clays, like the smectite clay or montmorillonite K-10 were employed two decades ago as heterogeneous catalysts for the alcoholysis of carbamates.[87] The resulting isocyanates are then formed at 180 °C using large amounts of solid catalyst (100 mg with respect to 0.6 mmol of isocyanate). Such high temperatures were necessary to desorb the alcohol product, especially bulkier ones. Yields of the isocyanate products were high in the case of light alcohol leaving groups (*e.g.* MeO–) and aromatic carbamates (Ph–NHCO–). The authors were able to produce MDI

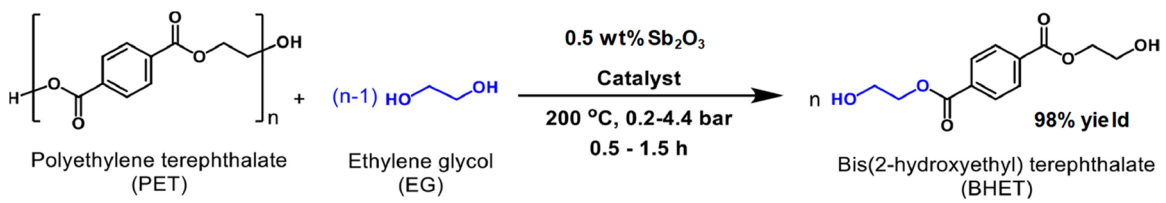

Scheme 14 Glycolysis of PET with EG in the presence of antimony(III) oxide as the catalyst. Reproduced with permission of ref. 86. Copyright (2022) Elsevier.

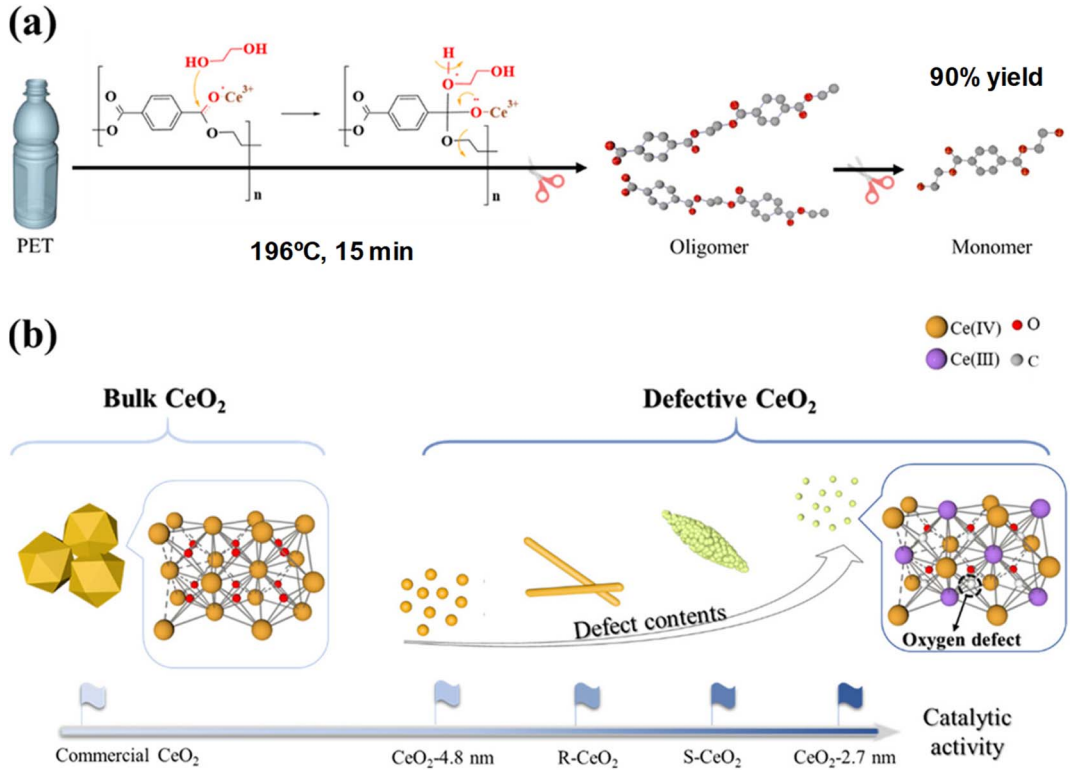

Scheme 15 (a) PET glycolysis (196 °C, 15 min) procedure over defective CeO_2 NPs. (b) Structures and catalytic activities of CeO_2 NPs with different morphologies. Reproduced with permission of ref. 56. Copyright (2022) American Chemical Society.

from MDPC (see Scheme 13 b) in decaline with *ca.* 70% yield after 24 h at 190 °C using a 25 wt% of catalyst. The reaction mechanism proposed requires an optimal number of Brønsted acid sites, such as those present in K-10 solid clay, to promote the alcoholysis avoiding excessive product absorption at the acid sites. In Scheme 16, the authors proposed the carbamate protonation by the Brønsted acid sites of K-10 and subsequent formation of the isocyanate by elimination of the amidic proton and the methoxy group. Both leaving groups are then combined in the form of the methanol byproduct (which is eliminated from the catalyst surface by heating to regenerate the active site).

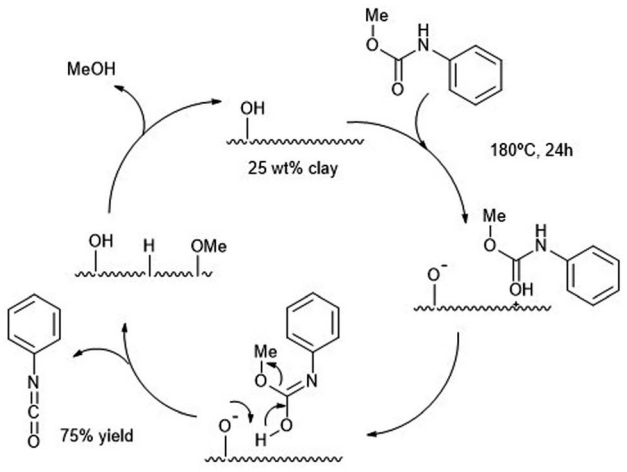

Scheme 16 Proposed mechanism for the decomposition of carbamates (180 °C, 24 h) into isocyanates at solid acid K-10 catalyst (25 wt%).

Co-precipitation of Zn, Mg and Al salts in a basic solution of carbonates and hydroxides resulted in the formation of layered double hydroxides.[57] The layered of (Mg–Zn)–Al–OH are spaced by 2.4 nm, and named as hydrotalcite or anionic clays (Scheme 17). PET glycolysis was carried out using a 10 : 1 mass ratio of the alcohol. The catalyst promotes a 95% conversion of PET and 80% selectivity to BHET was obtained after 3 h at 196 °C (see entry 21, Table 2). The active sites were both basic isolated O^{2-} ions, Mg^{2+}–O^{2-} pairs, and OH groups, as well as acid sites such as the Mg^{2+}, Al^{3+} and Zn^{2+} cations. On the one hand, the Lewis basic sites are responsible for the activation of the alcohol by interacting with hydroxyl groups. This is key for making the oxygen more nucleophilic for the attack on the carbonyl of the ester group in the PET. On the other hand, the Lewis acid sites withdraw the electron density of the oxygen atom. This makes the carbon atom of the group more electrophilic and susceptible to nucleophilic attack. The catalyst could be reused 4 times without significant loss in activity, the active site was regenerated by washing with water and the structure was maintained. Other authors prepared similar types of hydrotalcites but using Sn instead of Mg, and tested them as heterogeneous catalysts for PU degradation using DEG for 3 h at 190 °C.[58] Zn, Sn, Al hydrotalcites (HTCs) were employed in the glycolysis of flexible polyurethane foams. The conditions were: a PUF/DEG mass

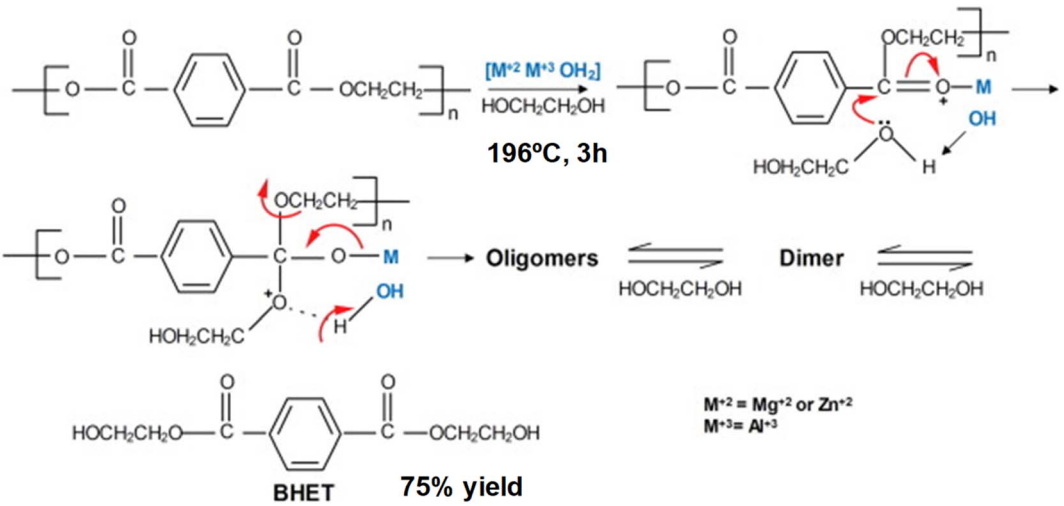

Scheme 17 PET glycolysis over Mg/Zn/Al hydrotalcites at 196 °C during 3 h. Reproduced with permission of ref. 57. Copyright (2016) Elsevier.

ratio of 1 : 5 and HTC/DEG of 0.001 (1.3% catalyst) and 66% of the polyol was recovered (see entry 22, Table 2).

Two-dimensional (2D) holey and ultrathin MnO_2/graphene oxide nanosheets (HGO = holey graphene oxide) were reported as catalysts for PET glycolysis (see Scheme 18).[88a] The synthetic process consisted of oxidative etching of graphite flakes (the graphene oxide solution) and a self-limiting redox reaction between $KMnO_4$ and Na_2SO_4 in water (as the MnO_2 solution). Both solutions were mixed at 80 °C for half an hour, and the MnO_2/HGO was isolated and dried. The optimal EG : PET ratio was 19 and the temperature was 200 °C, resulting in a quantitative BHET yield (100% conversion and yield) after 10 min using the MnO_2/HGO catalyst (0.01 wt%). Similar GO–Mn_3O_4 was prepared with similar oxidation method but under ultrasound conditions, requiring only tens of minutes under ambient conditions. However, very high temperatures (300 °C) were employed for PET glycolysis in this case.[88b]

A higher surface area was obtained for this material (247 m^2 g^{-1}) with respect to MnO_2 deposited in GO (69 m^2 g^{-1}). This was due to the holey GO support, which was key to its catalytic performance, maintaining its activity after 5 cycles. Even in the absence of the GO, ultrathin-exfoliated MnO_2 nanosheets exhibited an optimal performance for the glycolysis of PET. Indeed, 100% yield to BHET concerning bare MnO_2 (78% yield) was obtained (see entry 23, Table 2), permitting its use for 5 cycles without apparent loss of activity under reaction conditions (200 °C, 1 h, 0.1 wt% MnO_2 and 55 : 1 EG : PET weight ratio).[59] This proved the efficiency of the fluid dynamics-assisted intercalation and exfoliation method in the shear-exfoliation by K^+ intercalation between adjacent MnO_2 layers. The authors proposed a similar method to produce 2D-Fe nanosheets with high surface area (>200 m^2 g^{-1}) obtaining similar activity under similar reaction conditions.[89] In this case, the magnetic properties of the catalyst allow its simple separation and recycling five times without apparent loss in activity. It is worth mentioning that only a 10% yield was obtained in the absence of any catalyst. In this case, no active site was available to interact neither with the carbonyl or hydroxyl group from PET and EG, respectively.

4.2 Porous 3D frameworks

A synthesis of the isocyanate HDI by thermal decomposition of the carbonate HDC over Co_3O_4/ZSM-5 catalyst has been reported (Scheme 13 and 19).[90] The metal oxide was incorporated into the microporous medium pore zeolite by: (i) incipient wetness impregnation, (ii) PEG additive, or (iii) deposition

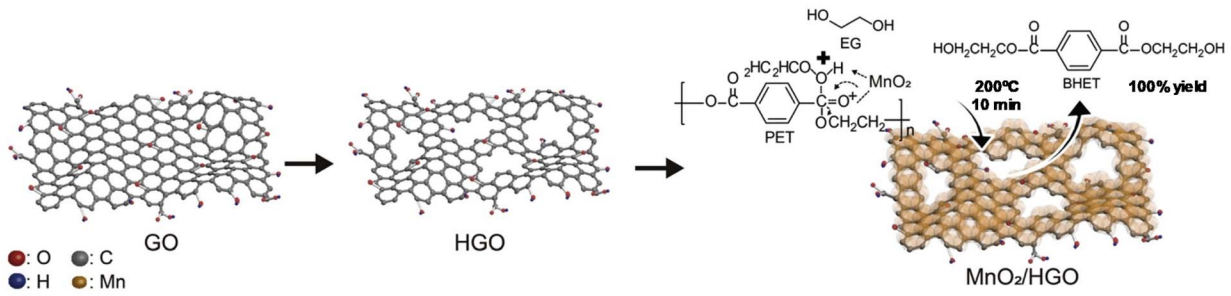

Scheme 18 Glycolysis of PET with EG (200 °C, 10 min) in the presence of MnO_2/HGO as the catalyst. Reproduced with permission of ref. 88a. Copyright (2021) Elsevier.

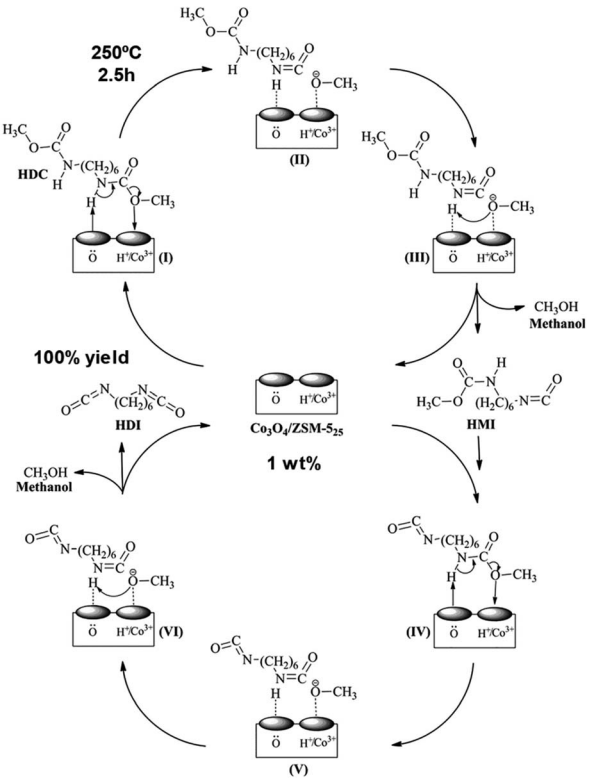

Scheme 19 A tentative mechanism for the thermal decomposition (250 °C) of HDC to HDI over Co_3O_4/ZSM-5 catalyst. Reproduced with permission of ref. 90. Copyright (2017) Elsevier.

precipitation with ammonia evaporation. A 6.5% HDC concentration in chlorobenzene, a 1 wt% Co_3O_4/ZSM-5 catalyst, under 250 °C temperature, 2.5 h time, 800 ml min^{-1} nitrogen flow rate and 1.0 MPa pressure was employed. The best performant catalyst was the one prepared with PEG additive (100% HDI yield), followed by one prepared by incipient wetness approach. The one prepared with ammonia was the less active one. The authors showed that catalytic activity is parallel to its acidity (measured by NH_3-TPD), surface cobalt content and surface lattice oxygen content. Both acidity and surface oxygen were key in the activation of the carbamate group during its decomposition, as shown in (Scheme 19). The same group reported a similar Zn-doped Co-ZSM-5 catalyst but using dioctyl sebacate as solvent (10 wt% concentration of HDC) at 250 °C for 60 min.[91] A yield of 84% of HDI was reported, maintaining its activity for 3 additional cycles. On the other hand, the hydrolysis of dimethyl terephthalate (DMT) was successfully achieved using a ZSM-5 containing niobium oxide sites.[92] The Brønsted acidity (in higher number with respect to the Lewis one) and a surface area (higher than 300 m^2 g^{-1}) were key to its catalytic activity. The reaction conditions employed were 5 wt% of catalyst with respect to DMT, 5 times more mass of water than DMT and 2 h of reaction. This resulted in a DMT conversion of 99% and a terephthalic acid yield of 94%, maintained during 5 additional reaction cycles.

Porous solids, such as the mesoporous silica SBA-15 were employed as host (or support) of zinc oxide nanoparticles resulting in active catalysts for PET degradation.[60] Using a PET/EG ratio of 1 : 4 and a catalyst (ZnO)/PET ratio of 0.05, a 100% conversion and 90% yield to BHET was obtained after 1 h at 200 °C (see entry 24, Table 2), similar to the performance of zinc acetate. The heterogeneous catalyst could be recycled 6 times, with a slight decrease in yield after the first 3 cycles (close to 80% BHET yield). However, a more pronounced decrease is observed afterward (down to 60% after the sixth recycle) due to loss of active components.

The zinc–organic framework known as MAF-6 (Metal-Azolate Framework-6) was an active catalyst in the degradation of PET with ethylene glycol. Using a 6 : 1 weight ratio at 180 °C for 4 h at atmospheric pressure, 92% PET conversion and 82% BHET yield was obtained (see Scheme 20, and entry 25, Table 2).[61] The high density of Lewis acid zinc sites, together with the excellent dispersibility of the substrates and catalyst allowed a better performance of the MOF with respect to traditional ZnO (28% PET conversion and 9% BHET yield) and Zn acetate (71% PET conversion and 52% BHET yield) under similar conditions (7.7 mmol Zn). The mechanism proposed assumes that the external surface active sites allow for the PET degradation into oligomers. The oligomers are transformed into dimers that have a sufficiently small size to penetrate the micropores of the MOF and be broken in the inner active sites of the crystal. Similar XRD patterns and low Zn leaching (3.7%) were observed after 5 recycles, maintaining the catalytic activity of the first cycle.

DES@ZIF-8 multifunctional catalyst was prepared from the mixture of the $ZnCl_2$/acetamide (with a molar ratio of 0.4/1) deep eutectic solvent (DES) with the ZIF-8 in a mass ratio of 1 : 4.[93] The XRD of the DES@ZIF-8 is significantly altered by the presence of the DES, although main characteristic peaks of ZIF-8 are still present. The composite was prepared by contacting both MOF and DES in ethanol, stirring at room temperature for 8 h and solvent evaporation. BHET yield was obtained by weighting the reaction mixture after such reaction time at 195 °C and 10 bars (EG : PET mass ratio = 5) and a work-up with hot water. A 100% conversion and 83% BHET selectivity were obtained after 30 min with the best performant Zn-DES@ZIF-8 (maintained during recycling), using only 0.4 wt%. of catalyst with respect to PET. In the case of bare ZIF-8, 73% BHET yield was obtained, which is not so far from the performance of the DES@ZIF-8 composite (only 10% more). The authors proposed that the zinc from the DES interacts with the carbonyl group of the PET. Moreover, the basic amino group of the acetamide does the same with the hydroxyl group of the EG in synergy with the Zn acid sites.

5 Chemo-enzymatic and biocatalytic depolymerization of plastic wastes

5.1 Biocatalytic degradation of PET wastes

The use of biological tools (*e.g.* microorganisms, enzymes, *etc.*) for plastic wastes degradation is a sustainable alternative to the chemical processes for eliminating plastic wastes under mild reaction conditions. This green approach is crucial for

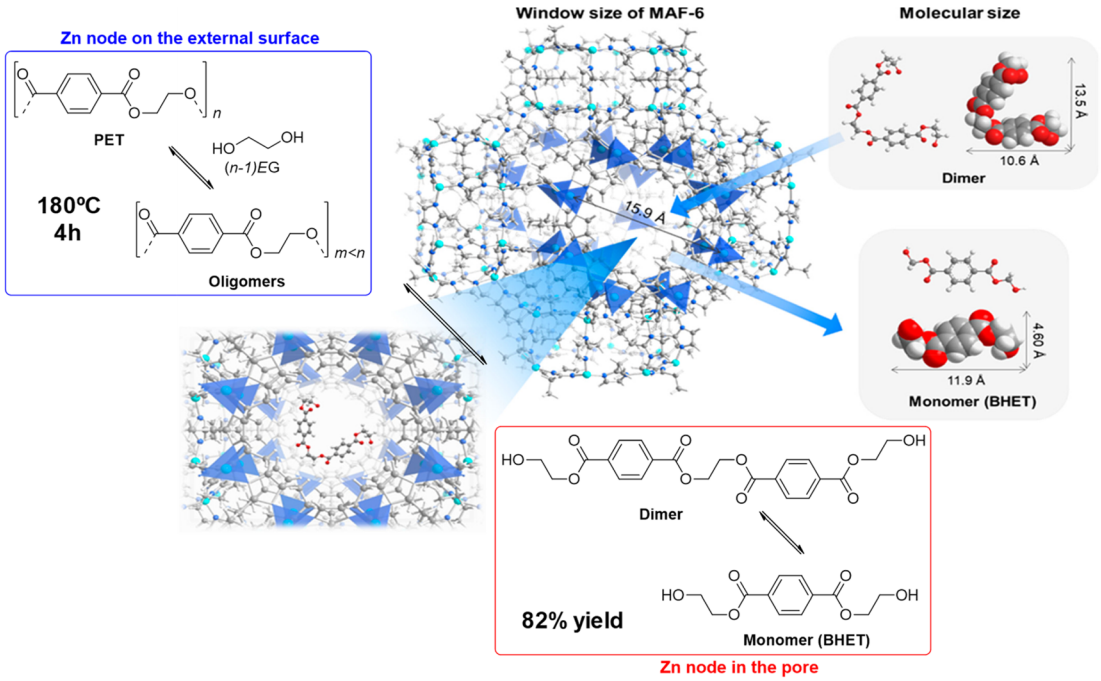

Scheme 20 Proposed mechanism for PU degradation at MAF-6 (180 °C, 4 h), together with size of both MAF-6 and, dimer and monomer (BHET). Adapted with permission of ref. 61. Copyright (2021) ACS.

developing new strategies for plastic recycling/upcycling, *via* depolymerization of recalcitrant materials into their constituent building blocks overcoming kinetic and thermodynamic limitations.[18,30] Recently, it has been reported the suitability of different enzymes for carrying out the degradation of plastic wastes (*e.g.* polyester, polyethylene, *etc.*) by using whole cells (*e.g.* bacterial, fungi, *etc.*) or enzymes (*e.g.* laccases, peroxidades, *etc.*).[94] Different hydrolases showed activity to break down bonds of the PET structure, providing terephthalic acid (TA), bis(2-hydroxyethyl)terephthalate (BHET), mono-(2-hydroxyehyl) terephthalic acid (MHET), and ethylene glycol (EG) (Scheme 21).[95]

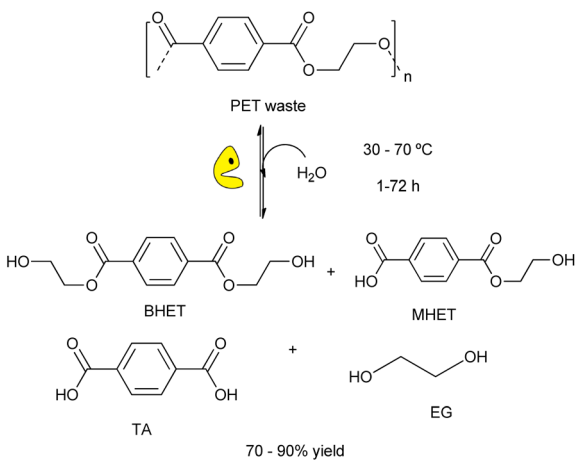

Scheme 21 Schematic representation of enzymatic hydrolysis of PET catalysed by engineered biocatalysts under mild conditions (water, RT-70 °C, 1–72 h).

As an alternative, Tournier *et al.*, developed a more sustainable enzymatic depolymerization of PET catalyzed by an engineered cutinase (instead of traditional chemical catalysts), reaching more than 90% postconsumer PET waste degradation after 10 h at 72 °C (entry 26, Table 2). In this study, they successfully demonstrated the reusability of the obtained products (*i.e.* terephthalic acid monomers) for resynthesizing a new PET under mild reaction conditions.[62a] It is worth mentioning that the French company CARBIOS is one of the most important examples of a sustainable industrial approach for the depolymerization of PET from waste plastic bottles.[62] Taking advantage of protein engineering technology, they have developed a PET depolymerase variant very useful for PET hydrolysis, achieving a productivity rate of 15.5 g L^{-1} h^{-1} of terephthalate, which corresponds to 200 g Kg_{PET}^{-1} using 2 mg_{enzyme} g_{PET}. In 2022, CARBIOS also demonstrated remarkable advances in PET depolymerization, providing a 97% depolymerization rate after 16 h at an industrial scale of 1000 L,[96] preventing more than 1.8 million tons of plastic foam and a considerable reduction of CO_2 emissions. Another important pathway for PET degradation consists in the development of suitable pretreatments of PET wastes to more enzyme-attackable foams which are necessary for PET recycling, demonstrating a remarkable improvement in the substrate accessibility (under microwave irradiation) to obtain PET powders. This approach allows the obtention of more suitable PET-derived constituents (compared to the original untreated PET) for subsequent biocatalytic steps with engineered PETases, achieving 78% yield after 2 h of microwave pretreatment and 1 h of enzymatic reaction at 30 °C (entry 27, Table 2).[63] Additionally, a physical pretreatment of PET has been

developed to provide a biodegradable form, based on amorphization and micronization towards more accessible substrate for PET hydrolases.[64]

It should also be noted that the expression and functionality of IsPETase^{Mut}, a variant of the PET-degrading enzyme from *Ideonella sakaiensis*, has been carried out. By optimizing expression systems in *E. coli*, two different approaches were recently developed: co-expressing with GroEL/ES chaperones and fusing the enzyme with NusA (entry 29, Table 2). Both strategies significantly increased the yield of soluble *Is*PETase^{Mut}, with NusA fusion, achieving the highest production at 80 mg L^{-1}, compared to 75 mg L^{-1} with GroEL/ES co-expression. While GroEL/ES did not affect the catalytic activity of the enzyme, the NusA fusion improved its properties by enhancing PET adsorption. Additionally, the product inhibition effect of TA on IsPETase was notably reduced with NusA-*Is*PETase^{Mut}, resulting in a weight loss of 19.6% for PET-NP. Despite the initial hydrolysis rate was slower, NusA-IsPETase^{Mut} demonstrated more effective long-term PET degradation, resulting in a 1.4-fold higher adsorption constant toward PET. These results indicate that NusA-*Is*PETase^{Mut} showed a significant long-term biodegradation behavior compared to *Is*PETase^{Mut} and *Is*PETase^{Mut} (GroEL/ES). Moreover, it is demonstrated that optimizing expression systems and fusion partners can significantly enhance enzyme production and performance, opening new opportunities for PET recycling technologies.[65a]

In the same context, the S238Y mutant, located near the catalytic triad, exhibited a significant enhancement in PET biodegradation, with a 3.3-fold increase in activity compared to the wild-type enzyme.[65b] In this study, circular PET films were washed with sterile deionized water and dried at room temperature for 48 h before enzymatic treatment. Then, the enzymatic reactions were assayed in buffer (50 mM glycine-sodium hydroxide, pH 9.4) at 30 °C for 72 h (see entry 30, Table 2). Notably, the structural modification improved the activity of the enzyme to break down highly crystallized PET (~31%), which is commonly found in commercial soft drink bottles. Furthermore, microscopic analysis revealed that mechanical stress on PET surfaces further improved enzyme efficacy by disrupting the crystalline structure (up to 3% loss of crystallinity).

Another strategy for the biocatalytic upcycling consists in the enzymatic depolymerization of PET through the addition of high concentrations of calcium ions (up to 1 M). This allows to carry out the hydrolysis catalysed by the engineered cutinase LCCICCG, exhibiting improved the thermal stability and activity in the presence of calcium cations, providing 84% PET conversion into calcium terephthalate ($CaTP \cdot 3H_2O$) at 80 °C for 12 h (entry 28, Table 2). Furthermore, the presence of calcium ions also reduced the amount of base required to maintain optimal pH levels. The recovered building blocks can be further used as raw material for the synthesis of value-added products (*i.e.* battery electrode production).[64]

Despite the difficulty of breaking down PET bonds due to its recalcitrant character, promising results for its biocatalytic depolymerization have also emerged using rational design and combinatorial mutagenesis. For instance, the development of a novel ICCG mutant RITK (D53R/R143I/D193T/E208K) cutinase showed excellent (whole-cell) biocatalytic activity, demonstrating the suitability of hydrolytic enzymes for plastic recycling.[66] The activity of a PET hydrolase was widely improved, allowing 90% PET depolymerization into 16.7 g L^{-1} h^{-1} of terephthalate monomer (for further reuse) using only 3 mg_{enzyme} $g^{-1}{}_{PET}$ (entry 31, Table 2). Alternatively, Quartinello *et al.* developed a synergistic chemo-enzymatic hydrolysis of PET from textile waste. In the first place, chemical hydrolysis at 250 °C and 40 bar was performed, reaching 85% conversion into both TA and small oligomers (entry 32, Table 2). Then, a second step of enzymatic hydrolysis of the obtained oligomeric compounds, catalysed by *Humicola insolens* cutinase (HiC), provided conversions of TA up to 100% (entry 33, Table 2).[67] However, one of the main challenges of the biocatalytic approaches is ensuring the operational stability of the biocatalysts under harsh industrial conditions (*e.g.* high temperatures) required for efficient degradation of large amounts of plastics. In this context, the development of new thermophilic microorganisms is needed for such conditions, although genetic engineering tools for designing these non-conventional host microorganisms are still under development.

5.2 Biocatalytic depolymerization of PU

As described above, PU is a class of synthetic polymer with huge environmental impact, which is obtained from the polycondensation reaction of a diisocyanate (*i.e.* toluene diisocyanate, TDI) and polyols, providing the characteristic recalcitrant and stable intra-molecular urethane bond.[97] Although recycling strategies based on circular chemistry concepts are also a key tool to achieve their depolymerization into valuable secondary materials, traditional chemical PU recycling processes require extreme reaction conditions (180–250 °C, 50 bar). This fact complicates the obtention of pure and useful monomers for further reuse, mainly due to uncontrolled side-products/reactions under these harsh conditions. A sustainable alternative to the traditional chemical hydrolysis of PU is the biocatalytic degradation under milder conditions, reducing the operational costs and the use of toxic compounds. In general, the biocatalytic degradation of PU involves the use of enzymes (*i.e.* esterases, proteases, ureases, *etc.*) expressed in fungi and bacteria to produce alcohols, amines, and CO_2 (Scheme 22).[98]

Despite the xenobiotic, recalcitrant, and stable nature of PU wastes, few examples of selective biological catalysts have reported for the partial biodegradation of the polyester-polyurethane bonds.[99] For instance, the treatment of ultrathin PU using urease and papain enzymes for a long time (1–6 months), achieved a slight change in the PU surface.[100] These slight variations and the enormous difficulty of carrying out biocatalytic processes for polyurethane hydrolysis could be explained, not only because of the recalcitrant character and the stability of PU, but also because of the potent inhibitor effect of carbamate and thiocarbamate compounds on the serin proteases and hydrolases. Besides this inhibiting effect, different classes of enzymes have been reported for PU degradation (*e.g.* esterases, proteases, lipases).[101] For example, a *Trametes versicolor* laccase was evaluated as biocatalysts on four representative polyester- and polyether-based PU wastes, obtaining

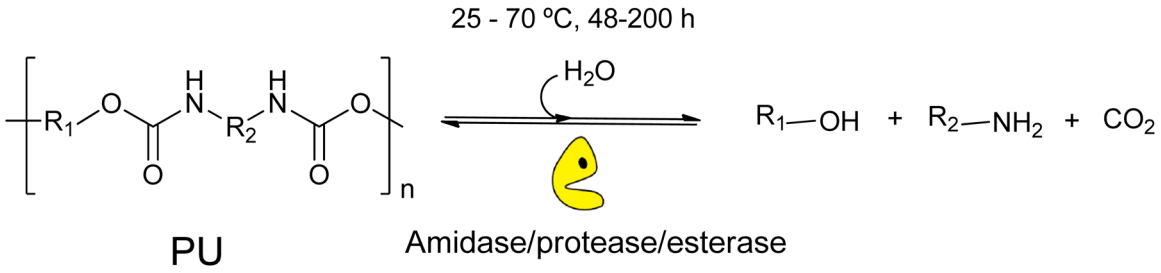

Scheme 22 Schematic representation of enzymatic hydrolysis of PU catalysed by amidase, protease, or esterase under mild conditions (water, RT-70 °C, 48–200 h).

a remarkable reduction in the molar masses after 18 days of incubation at 37 °C (entry 34, Table 2).[68] Alternatively, *Humicola insolens* cutinase were able to hydrolyse PU-polyester films after 168 h at 50 °C, achieving only 42% yield (entry 35, Table 2).[69] In addition, Schmidt *et al.* studied the degradation of the polyester PU Impranil DLN by the polyester hydrolases LC cutinase (LCC), TfCut2, Tcur1278 and Tcur0390, reaching up to 4.9% weight loss in polyester PU (by turbidimetric assay) after 200 h reaction at 70 °C (entries 36 and 37, Table 2).[70]

On the other hand, thermostable polyester hydrolases also proved to be suitable biocatalysts for the hydrolysis of polyester PU. For instance, lipases have been an interesting tool to perform the hydrolysis of commercially available solid poly(-ester)urethanes. *Candida rugosa* lipase was used to hydrolyze polyester PU particles in an aqueous medium, which led to valuable ethylene glycol byproduct, with a generation rate of 0.12 mg L^{-1} min^{-1} (entry 38, Table 2).[71] However, most strategies of biocatalytic hydrolysis of PU require the development of two-step chemo-enzymatic approaches, such as a first step of the depolymerization of polyether-polyurethane using a glycolysis reaction with DEG catalysed by tin(II)-2-ethylhexanoate at high temperature (*i.e.* >200 °C) (entry 39, Table 2). However, this approach achieved low molecular weight dicarbamates, carbon dioxide, and toluene diamines (TDA). On the contrary, the second biocatalytic hydrolysis step, allowed up to 100% conversion of the obtained dicarbamates, using an engineered urethanase for 48 h at 70 °C (entry 40, Table 2).[72]

Different enzymes (*i.e.* lipase, urease, protease, *etc.*) have been demonstrated as high-performant biocatalysts for the hydrolysis toluene-based urethane model compounds (*i.e.* bis(2-methoxyethyl) (4-methyl-1,3-phenylene)dicarbamate), using organic solvents (*i.e.* ethylene glycol or solketal) or, ionic liquids (*e.g.* 1-butyl-3-methylimidazolium bis(trifluoromethylsulfonyl) imide, [C_4mim][NTf_2]) as a reaction media.[102] However, most of the enzymes were unable to catalyse the hydrolysis of the carbamate bonds in pure water. This was due to the insolubility of these di-urethane compounds in water, which was improved (up to 31.6 mU mg^{-1} for the urease case) in a mixture of solketal : water (90 : 10, v/v) reaction media. Alternatively, when hydrophobic ILs were used as reaction medium, the urease activity increased twofold (74.1 mU mg^{-1}). The highest specific activity for the hydrolysis of these urethane compounds were obtained by combining lipase and urease biocatalysts in a IL : solketal : H_2O (70 : 25 : 5, v/v/v) reaction medium after 48 h at 60 °C. These results demonstrated a sustainable biocatalytic strategy for the hydrolytic depolymerization of polyurethane foam wastes.

Another bioprocess for PU degradation is based on the use of abundant microorganisms (*i.e.* fungi and bacteria) able to degrade synthetic plastics.[103–105] For instance, Su *et al.* demonstrated the use of microbial consortia in the biodegradation of PU wastes, as these microbes were able to use PU as the sole carbon source and accumulate high biomass within 1 week. Extracellular enzyme analyses showed that the consortia secreted esterase and urease, which could be potentially involved in the degradation of PU, although the metabolic pathway of the degradation is still unknown.[106] On the other hand, different polyester-polyether urethane degrading yeasts were isolated, resulting in two new strains of *Exophilia* sp. NS-7 and *Rhodotorula* sp. NS-12. The results showed that *Exophilia* sp. NS-7 was esterase, protease, and urease positive, and *Rhodotorula* sp. NS-12 could produce esterase and urease, and both strains were able to degrade Impranil® as a carbon source, providing a growth rate of 4–6 and 8–12 days, respectively.[107] However, the previously mentioned concept of recovery, recycling and reuse (3R) of the compounds does not completely apply, since the microorganisms use PU wastes as nutrients, preventing the concept of a circular economy.[108] This drawback can be explained because the structure of the PU residue is not broken down to provide valuable chemical building blocks, or useful constituents of the original polymer to offer promising routes towards life-cycle products. In fact, the microbiological elimination of solid plastic wastes by oxidative metabolic pathway transformations just consists of its full degradation into the most disseminated waste molecule, such as CO_2. In this way, the (bio)catalytic breakdown of plastic wastes into their building blocks for further reuse will always be a more sustainable solution than biological digestion.

6 SWOT analysis: chemocatalytic *vs.* biocatalytic processes for recycling polymeric waste (PET and PUs)

Once the key examples and current tools have been reviewed in the field of catalytic recycling, a Strengths, Weaknesses, Opportunities, Threats (SWOT) analysis provides a comprehensive overview of the relative strengths, weaknesses, opportunities, and threats associated with different catalytic approaches.

This analytical framework is crucial for understanding the advantages and limitations of both chemocatalytic and biocatalytic methods, offering insights into their practical impacts. Table 2 shows a compilation of the characteristics of the different catalytic processes analyzed in this work on the depolymerization of polyester and polyurethane waste. Both chemocatalytic and biocatalytic approaches have their unique strengths and challenges. Strategic investments in research and development, as well as thoughtful consideration of environmental impacts, economic factors, and technological capabilities, are essential for advancing sustainable recycling technologies. By assessing the positive aspects and current shortcomings, the SWOT analysis facilitates a critical examination of each approach. Furthermore, it helps identify potential future opportunities and threats, which can guide strategic planning and innovation in the field. This kind of analysis is vital for steering future research directions and improving the technologies involved in polymer recycling, ensuring that they are more efficient, sustainable, and adaptable to varying waste stream conditions. Scheme 23 depict the SWOT analysis for both approaches here evaluated.

6.1 Chemocatalytic systems

In the first place, the SWOT for the field of chemocatalysis for polymer recycling is presented analysing the examples highlighted through review and current research trends. This comprehensive approach has outlined the current capabilities and future directions of chemocatalytic technologies in addressing the challenges associated with polymer waste.

6.2 Strengths

6.2.1 Technological maturity. In general, chemocatalytic processes are well-established with proven industrial applicability and scalability. Their integration into existing industrial setups is facilitated by the extensive experience and technical knowledge accumulated from the production of bulk chemicals. This background supports the adaptation and application of these processes in the recycling sector, allowing for a smoother transition and implementation in dealing with polymeric wastes. By leveraging the established chemical engineering principles and catalytic technologies, it becomes feasible to apply these methods effectively to the challenges of recycling polymers, enhancing both the efficiency and sustainability of these operations.

6.2.2 Efficiency. Chemocatalytic processes are highly efficient due to their ability to offer faster reaction times and higher yields under optimized conditions. This efficiency is critical for enhancing the throughput of these systems, making them well-suited for large-scale operations. The capability to process large volumes of material quickly and with high yield translates into greater productivity and economic viability in industrial recycling applications. By optimizing reaction conditions, such as temperature, pressure, and catalyst concentration, these processes can maximize output and reduce waste, further improving their feasibility for widespread industrial use in recycling polymers like PET and PU.

6.2.3 Robustness. Chemocatalysts are notably robust, capable of withstanding harsher operational conditions and handling a broader range of substrates, which is particularly beneficial in the recycling of polymers like PET and PU. This robustness helps to mitigate the challenges associated with feedstock variability, allowing these catalysts to effectively process different qualities and compositions of polymeric waste. This adaptability ensures more consistent recycling outcomes, enhances the efficiency of the process, and reduces potential downtime or additional processing steps that might be required to pre-treat variable feedstocks. Such properties make chemocatalysts highly suitable for the diverse and often unpredictable nature of waste streams encountered in large-scale recycling operations.

6.3 Weaknesses

6.3.1 Environmental impact. The environmental impact of chemocatalysis, particularly concerning the use of high temperatures and potentially hazardous chemicals such as specific ligands or metals, is a significant concern. These elements raise issues regarding energy consumption and the environmental fate of the catalysts used. To mitigate these impacts, it is crucial to design catalysts that utilize widely available, low-toxicity materials. The selection of less hazardous ligands and metals not only addresses environmental safety concerns but also aligns with the principles of green chemistry. This approach emphasizes the reduction of chemical hazards and resource efficiency, thereby reducing the overall ecological footprint of catalytic processes.

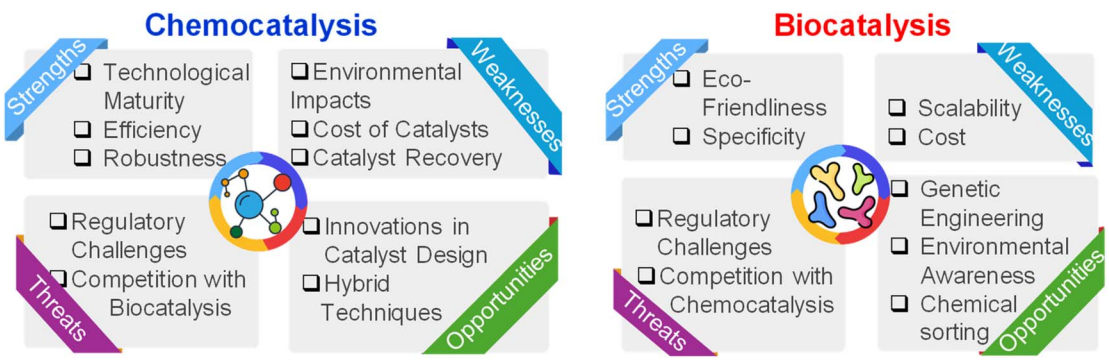

Scheme 23 SWOT analysis of chemo- *vs.*-bio-catalysis approaches for the degradation of (polyester/polyurethane) plastic waste.

Implementing such environmentally friendly strategies involves selecting catalyst materials that are abundant and benign, while still maintaining the efficiency and effectiveness required for industrial applications. Moreover, optimizing the catalytic process to operate at lower temperatures can significantly reduce energy consumption, further enhancing the sustainability of the process. These measures are vital for developing more sustainable catalytic technologies that are safer for both the environment and human health.

6.3.2 Cost of catalysts. The cost of catalysts, particularly transition metals and other specialized catalytic materials, is a significant consideration in the economic viability of chemocatalytic processes. These materials can be expensive and are subject to market fluctuations, which may significantly impact the cost-effectiveness of industrial processes. This variability can pose a challenge to maintaining consistent production costs and process affordability. To manage these challenges, research and development efforts often focus on finding more abundant or less expensive alternatives that can perform similarly to costlier materials.

6.3.3 Catalyst recovery. Challenges in catalyst recovery and recycling can lead to additional costs and environmental burdens. Improving the efficiency and recyclability of catalysts can also help reduce the overall amount of material required and extend the lifecycle of the catalysts, thereby decreasing the impact of price volatility. Developing catalysts that can be easily regenerated and reused, such as integrating the metal in a solid (either dense or open/porous) framework, without significant loss of activity is another way to minimize the ongoing costs associated with raw materials in chemocatalysis. These strategies are crucial for making catalytic processes more sustainable and economically feasible in the long term.

6.4 Opportunities

6.4.1 Innovations in catalyst design. Developing more efficient and selective catalysts can significantly improve yields while minimizing unwanted by-products. This not only boosts the process's environmental footprint but also its economic viability. Traditional metal-based catalysts, while robust and technologically proven, may sometimes fall short in terms of selectivity or require harsh operational conditions. In contrast, advanced metal–organic hybrids, especially metal–organic frameworks (MOFs), present exciting opportunities to overcome these limitations. MOFs are known for their highly ordered, porous structures which can be engineered to contain well-dispersed active sites. These sites offer enhanced activity and stability, potentially allowing for operations under milder conditions — lower temperatures and pressures — which are less energy-intensive and more environmentally friendly. The rational engineering of these hybrid catalysts involves designing frameworks that not only accommodate but also stabilize the active metal sites, ensuring that they are accessible and effective during the reaction. This can lead to significant improvements in the efficiency of polymer degradation processes like solvolysis.

6.4.2 Hybrid techniques. Integrating chemocatalysis with other recycling methods, such as mechanochemistry, microwave-assisted reactions, or using ionic liquids as solvents, can create hybrid techniques that enhance polymer recycling. These hybrid approaches leverage the unique strengths of each individual method to achieve polymer recoveries that are not attainable by any single technique alone. By combining different methodologies, researchers and engineers can overcome the limitations of traditional recycling methods, enhancing both the environmental and economic viability of polymer recycling processes.

6.5 Threats

6.5.1 Regulatory challenges. The increasingly harsh environmental regulations pose significant regulatory challenges to the chemocatalysis industry, particularly impacting the use of certain specific catalysts and solvents, especially those that are toxic, hazardous, persistent, or bioaccumulative. It is essential to find safer alternatives to meet regulatory standards and enhance process efficiency. These regulatory landscapes require continuous monitoring and adaptation, as well as proactive engagement with regulatory developments to ensure compliance and maintain operational efficiency.

6.5.2 Competition with biocatalysis. Advances in biocatalysis could shift industry preference towards more environmentally friendly and potentially cost-effective depolymerization methods based on biocatalysts. While this competition can be a threat for traditional chemical processes, it also drives innovation, prompting us and the industry to develop in cleaner, more sustainable technologies. This competitive pressure can ultimately lead to better environmental outcomes and more efficient recycling processes.

6.5.3 Biocatalytic systems. The highlighted advances in biocatalysis are positioning it as a formidable competitor to traditional chemocatalytic processes in the field of polymer recycling. This is the SWOT analysis for this kind of systems.

6.6 Strengths of biocatalysis

6.6.1 Eco-friendliness. Biocatalysts, which facilitate reactions under milder conditions compared to traditional chemocatalysts, offer significant environmental benefits. Operating at ambient temperatures and pressures, biocatalysis drastically reduces the energy consumption and greenhouse gas emissions associated with the recycling process. Such eco-friendly attributes make biocatalysis an attractive option for process aiming to enhance their sustainability practices.

6.6.2 Specificity. Enzymes are highly specific. This specificity ensures that enzymes catalyze only their target reactions, reducing the likelihood of unwanted by-products. Consequently, processes that utilize enzymes typically yield cleaner products and generate fewer side reactions compared to conventional chemocatalytic methods. This characteristic not only enhances the quality of the final product but also simplifies the purification process, leading to cost savings and less environmental burden from waste products.

6.7 Weaknesses

6.7.1 Scalability. Scaling biocatalytic processes to industrial levels presents significant challenges primarily due to issues with

enzyme stability and activity under large-scale conditions. Another scalability challenge is the cost associated with producing large quantities of biocatalysts. Enzyme production often involves complex biotechnological processes that can be expensive to operate at a large scale. Furthermore, integrating these bioprocesses into existing industrial setups requires significant capital investment in specialized equipment and technologies.

6.7.2 Cost. The economic viability of biocatalytic processes is often challenged by the high costs associated with enzyme production and purification. Producing enzymes in quantities sufficient for industrial applications typically involves complex biotechnological processes, including genetic engineering and fermentation, which require specialized equipment and expertise. Additionally, ensuring that these enzymes are of the necessary purity for effective use can involve elaborate and costly purification steps. To solve this, it is needed to develop more robust enzymes, optimizing operational conditions, and engineer cost-effective enzyme production and recovery methods.

6.8 Opportunities

6.8.1 Advances in genetic engineering. Advances in genetic engineering are significantly enhancing the landscape of biocatalysis, making it a more viable and competitive option in various industrial processes. By improving the stability, efficiency, and cost-effectiveness of enzymes, genetic engineering allows for broader applications and scalability of biocatalytic methods.

6.8.2 Growing environmental awareness. Increased consumer and regulatory demand for sustainable processes may drive further development and adoption of biocatalytic recycling methods.

6.8.3 Chemical sorting. The highly specific nature of enzymes offers a compelling advantage in the recycling of polymers through selective separation and recovery. This specificity enables enzymes to selectively depolymerize certain types of polymers in mixtures containing various polymers, without affecting others. This process can function similarly to a chemical sorting mechanism, allowing for the sequential breakdown and separation of polymers based on their chemical composition and reducing the need for extensive physical sorting and pre-treatment processes typically required in conventional recycling methods, potentially lowering overall processing costs and increasing efficiency.

6.9 Threats

6.9.1 Technological limitations. The technological limitations of enzymes, particularly in terms of performance and lifespan under industrial conditions, pose significant challenges for their broader application in various sectors. These limitations can restrict the scope of enzyme applications, particularly in high-volume and high-intensity industrial processes where robust and durable solutions are essential.

6.9.2 Market competition. The competition from well-established chemocatalytic processes presents a formidable challenge to the growth of biocatalytic methods in the market. Chemocatalysis has a strong foothold due to its long history of industrial application, proven scalability, and ongoing innovations that continue to enhance its efficiency and applicability across various sectors.

7 Technology readiness level of the (bio)catalytic approaches at industrial level

Catalytic and biocatalytic recycling methods for PET and PU waste vary significantly in technological readiness. These technologies generally span Technology Readiness Levels (TRL) 3 to 8, depending on the type of polymer and catalyst used. Catalytic methods for PET and PU recycling are often found in academic settings at lower TRLs (up to TRL 3), focusing on early-stage research and development of the catalyst. In contrast, several examples have progressed to pilot-scale or even commercial deployment, reaching TRLs 8–9. The transition from initial TRLs to full-scale industrial application requires addressing challenges related to efficiency, cost, scalability, and maintaining environmental compliance and product quality.

In this context, catalytic glycolysis and hydrolysis of PU have advanced from laboratory research to pilot and industrial-scale applications, showing promising potential for the chemical recovery of polyols from PU waste.[109] Companies like Repsol,[110] and DOW chemicals,[111] operate full-scale plants dedicated to PU recycling, showcasing the commercial viability of these technologies. However, biocatalytic approaches for PU recycling remain at a lower TRL (<4), mainly confined to laboratory-scale demonstrations and early development stages.

On the other hand, both catalytic and biocatalytic processes for PET hydrolysis have reached higher TRLs, bridging the gap from novel academic developments to full-scale industrial applications. Catalytic hydrolysis methods, utilizing zinc or other metal catalysts, are implemented by companies such as Ioniqa Technologies,[112] Loop Industries,[113] and Indorama Ventures,[114] at commercial levels. These methods efficiently depolymerize PET into monomers that can be reused in new production cycles.

Biocatalytic methods, particularly those involving enzymes like PETase, have shown significant promise, reaching pilot and industrial scales. Carbios is a leader in this field, having developed advanced enzymatic recycling techniques that are now operational at industrial levels, paving the way for more sustainable PET recycling processes. Carbios uses engineered enzymes specifically designed to degrade PET, demonstrating the efficiency and scalability of biocatalytic methods, especially in industries like packaging and textiles. This dual approach of catalytic and biocatalytic recycling is setting new standards for circular economies in polymer recycling, highlighting the potential for broader industrial application.[115]

8 Conclusions

Plastic waste represents a significant challenge in modern society, necessitating a multi-faceted approach to management and recycling. Industries producing polyester and polyurethane must adopt circular chemistry protocols to reintegrate waste

back into their production chains, a crucial step for environmental preservation and achieving the Sustainable Development Goals (SDGs) set by the United Nations. The adoption of biodegradable plastics and renewable raw materials marks a strategic advancement in reducing environmental impact. However, the creation of biodegradable waste can lead to a loss of economic value and contribute to CO_2 emissions through decomposition processes.

This review thoroughly examines catalytic recycling methods, particularly chemocatalytic and biocatalytic strategies for breaking down polyester and polyurethane waste. The analysis reveals a complex balance of strengths, weaknesses, opportunities, and threats associated with these technologies. Chemocatalysis, while robust and efficient, faces environmental and cost challenges. On the other hand, biocatalysis offers an eco-friendlier alternative with greater specificity and lower energy demands, though it struggles with scalability and high operational costs.

Significant advancements in the field underline the need for strategic research and development investments to improve the sustainability and economic viability of recycling technologies. Innovations in catalyst design that can operate under milder conditions and enhance selectivity and stability are particularly promising. These could greatly reduce the environmental impact and improve the economic feasibility of these processes. Traditional metal-based catalysts are well-established, but newer metal–organic hybrids and biocatalysts are still developing within the context of plastic recycling. For instance, Zn-based catalysts are favored for their biocompatibility and stability, with PET frequently used in degradation tests. The review also discusses the high reaction temperatures—often above 150 °C—required in many processes, which lead to significant energy consumption and by-product formation. Efforts to use water as a solvent for polymer hydrolysis under milder conditions are recommended. Biocatalysts, which can operate under less harsh conditions such as temperatures below 80 °C without pressure or organic solvents, present a viable but currently costly option. Future developments may reduce these costs and broaden the industrial applicability of biocatalysts in recycling. The development of hybrid materials (MOF) and advancements in genetic engineering and materials science could significantly advance both chemocatalysis and biocatalysis, making them more adaptable to various industrial applications. Such progress is vital for aligning with global sustainability goals and transitioning towards a circular economy in polymer production and waste management.

Finally, the future of polymer recycling relies heavily on our ability to develop catalytic processes that meet the technical demands of polymer degradation while aligning with environmental regulations and economic realities. Insights from this review are set to guide future research directions and enhance the technologies involved in polymer recycling, ensuring greater efficiency, sustainability, and adaptability to the dynamics of waste stream conditions.

Data availability

No primary research results, software or code have been included and no new data were generated or analysed as part of this review.

Author contributions

Francisco G. Cirujano: conceptualization, formal analysis, funding acquisition, investigation, methodology, supervision, writing – original draft, writing – review & editing; Rocio Villa: conceptualization, data curation, formal analysis, investigation, methodology, writing – original draft, writing – review & editing; Rebeca Salas: conceptualization, data curation, formal analysis, investigation, methodology, validation, visualization, writing – original draft, writing – review & editing; Miguel Maireles: investigation, writing – review & editing; Nuria. Martin, data curation, formal analysis, investigation, writing – review & editing; Belen Altava: data curation, funding acquisition, formal analysis, investigation, writing – review & editing; Pedro Lozano: conceptualization; formal analysis, funding acquisition, investigation, methodology, writing – review & editing; Eduardo García-Verdugo: conceptualization; formal analysis, funding acquisition, investigation, methodology, writing – review & editing.

Conflicts of interest

There are no conflicts to declare.

Acknowledgements

This work has been partially supported by MICINN-FEDER-AEI 10.13039/501100011033 (PID2021-124695OB-C21/C22, PID2022-142897OA-I00 and PDC2022-133313-C21/C22), MICINN – European Union Next Generation EU-PRTR (TED2021-129626B-C21/C22), and Fundación SENECA (21884/PI/22) grants. F. G. C. and N. M. acknowledge the "Ramon y Cajal" contract with code RYC2020-028681-I and RYC2021-033167-I funded MCIN/AEI/10.13039/501100011033 and by "ESF investing in your future", "European Union NextGenerationEU/PRTR". FGC thank Generalitat Valenciana (CISEJI/2023/78). UJI is acknowledged for the project UJI-2023-03.

References

1 PlasticsEurope, Plastics – the Facts 2022, 2022, accessed 19 Dec 2023, https://plasticseurope.org/wp-content/uploads/2022/10/PE-PLASTICS-THE-FACTS_V7-Tue_19-10-1.pdf.
2 X. Yuan, X. Wang, B. Sarkar and Y. S. Ok, *Nat. Rev. Earth Environ.*, 2021, **2**, 659–660.
3 A. L. Andrady and M. A. Neal, *Philos. Trans. R. Soc., B*, 2009, **364**, 1977–1984.
4 W. T. Hsu, T. Domenech and W. McDowall, *Clean. Environ. Syst.*, 2021, **2**, 100004.
5 P. Industry Association: Flexible bag and film division, https://www.plasticsindustry.org/supply-chain/processors/flexible-film-and-bag-division, 08/05/2023.
6 L. Mishnaevsky Jr, K. Branner, H. Norgaard Petersen, J. Beauson, M. McGugan and B. F. Sorensen, *Materials*, 2017, **10**, 1285.
7 J. Boucher, G. Billard, E. Simeone and J. Sousa, *The Marine Plastic Foot Print: towards a Science-Based Metric for*

Measuring Marine Plastic Leakage and Increasing the Materiality and Circularity of Plastic, IUCN Publication, Gland, 2020, DOI: 10.2305/iucn.ch.2020.01.en.

8 OECD, *Global Plastics Outlook: Economic Drivers, Environmental Impacts and Policy Options*, OECD Publishing, Paris, 2022.

9 E. Butler, G. Devlin and K. McDonnell, *Waste Biomass Valorization*, 2011, **2**, 227–255.

10 K. Zheng, Y. Wu, Z. Hu, S. Wang, X. Jiao, J. Zhu, Y. Sun and Y. Xie, *Chem. Soc. Rev.*, 2023, **52**, 8–29.

11 (*a*) H. Sardon and P. Dove Andrew, *Science*, 2018, **360**, 380–381; (*b*) R. Geyer, J. R. Jambeck and K. L. Law, *Sci. Adv.*, 2017, **3**, e1700782.

12 R. A. Sheldon and D. Brady, *ChemSusChem*, 2022, **15**, e202102628.

13 P. Lozano and E. García-Verdugo, *Green Chem.*, 2023, **25**, 7041–7057.

14 European Commission, *The Implementation of the Circular Economy Action Plan*, COM, 2019, p. 190.

15 Plastic Europe: Plastics-the Facts 2020. An analysis of European latest plastics production, demand and waste data, 2020, https://www.plasticseurope.org/en/resources/market-data.

16 J. Garcia-Martinez, *Angew. Chem., Int. Ed.*, 2021, **60**, 4956–4960.

17 Chemistry can help make plastics sustainable — but it isn't the whole solution, *Nature*, 2021, vol. 590, pp. 363–364, DOI: 10.1038/d41586-021-00391-7.

18 H. J. Thamhain, *Paper presented at Project Management Institute Annual Seminars & Symposium*, Houston, TX Newtown Square, PA, Project Management Institute, https://www.pmi.org/learning/library/phase-gate-processes-promising-complex-547, accessed: December 2023.

19 C. Hussong, J. Langanke and W. Leitner, *Green Chem.*, 2020, **22**, 8260–8270.

20 F. R. Wurm, S. Spierling, H. J. Endres and L. Barner, *Macromol. Rapid Commun.*, 2020, **41**, 2000351.

21 (*a*) T. Keijer, V. Bakker and J. C. Slootweg, *Nat. Chem.*, 2019, **11**, 190–195; (*b*) H. Mutlu and L. Barner, *Macromol. Chem. Phys.*, 2022, **223**, 2200111.

22 National Science Foundation Centre for Sustainable Polymers, https://csp.umn.edu/sustainable-polymers-101/#1612191883762-e1fcd6cf-bd73, accessed: December 2021.

23 Ellen MacArthur Foundation – What is a circular economy, https://ellenmacarthurfoundation.org/topics/circular-economyintroduction/overview, accessed: December 2021.

24 I. A. Ignatyev, W. Thielemans and B. Vander Beke, *ChemSusChem*, 2014, **7**, 1579–1593.

25 M. Solis and S. Silveira, *Waste Manag.*, 2020, **105**, 128–138.

26 S. M. Al-Salem, P. Lettieri and J. Baeyens, *Prog. Energy Combust. Sci.*, 2010, **36**, 103–129.

27 C. Baillie, D. Matovic, T. Thamae and S. Vaja, *Resour., Conserv. Recycl.*, 2011, **55**, 973–978.

28 (*a*) D. S. Achilias, A. Giannoulis and G. Z. Papageorgiou, *Polym. Bull.*, 2009, **63**, 449–465; (*b*) A. J. Hadi, G. F. Najmuldeen and K. Bin Yusoh, *J. Polym. Eng.*, 2013, **33**, 471–481.

29 (*a*) E. J. Cho, S. Lee, S. J. Oh, M. Han, Y. S. Lee and C. N. Whang, *Phys. Rev. B: Condens. Matter Mater. Phys.*, 1995, **52**, 16443–16450; (*b*) A. L. Andrady, *Plastics and the Environment*, John Wiley & Sons, New York, 2003; (*c*) Z. Jia, L. Gao, L. Qin and J. Yin, *RSC Sustainability*, 2023, **1**, 2135–2147; (*d*) K. Ghosal and C. Nayak, *Mater. Adv.*, 2022, **3**, 1974–1992; (*e*) A. Bohre, P. Ram Jadhao, K. Tripathi, K. Kishore Pant, B. Likozar and B. Saha, *ChemSusChem*, 2023, **16**, e202300142.

30 (*a*) B. Agostinho, A. J. D. Silvestre and A. F. Sousa, *Green Chem.*, 2022, **24**, 3115–3119; (*b*) M. Imran, B.-K. Kim, M. Han, B. G. Cho and D. H. Kim, *Polym. Degrad. Stab.*, 2010, **95**, 1686–1693; (*c*) Z. Shen, Z. Jia, K. Yu, J. Xie, L. Qin, L. Gao, B. Li, X. Wang and J. Yin, *Process Saf. Environ. Prot.*, 2024, **188**, 230–238.

31 L. D. Ellis, N. A. Rorrer, K. P. Sullivan, M. Otto, J. E. McGeehan, Y. Roman-Leshkov, N. Wierckx and G. T. Beckham, *Nat. Catal.*, 2021, **4**, 539–556.

32 M. Chu, Y. Liu, X. Lou, Q. Zhang and J. Chen, *ACS Catal.*, 2022, **12**, 4659–4679.

33 A. Bohre, P. R. Jadhao, K. Tripathi, K. K. Pant, B. Likozar and B. Saha, *ChemSusChem*, 2023, **16**, e202300142.

34 B. Agostinho, A. J. D. Silvestre, J. A. P. Coutinho and A. F. Sousa, *Green Chem.*, 2023, **25**, 13–31.

35 S. C. Kosloski-Oh, Z. A. Wood, Y. Manjarrez, J. P. de los Rios and M. E. Fieser, *Mater. Horiz.*, 2021, **8**, 1084–1129.

36 I. Olazabal, E. J. Luna Barrios, S. De Meester, C. Jehanno and H. Sardon, *ACS Appl. Polym. Mater.*, 2024, **6**(7), 4226–4232.

37 E. Luna, I. Olazabal, M. Roosen, A. Mueller, C. Jehanno, M. Ximenis, S. de Meester and H. Sardon, *Chem. Eng. J.*, 2024, **482**, 148861.

38 I. Olazabal, E. Luna, S. De Meester, C. Jehanno and H. Sardon, *Polym. Chem.*, 2023, **14**, 2299–2307.

39 I. Olazabal, A. González, S. Vallejos, I. Rivilla, C. Jehanno and H. Sardon, *ACS Sustain. Chem. Eng.*, 2023, **11**, 332–342.

40 R. Heiran, A. Ghaderian, A. Reghunadhan, F. Sedaghati, S. Thomas and A. H. Haghighi, *J. Polym. Res.*, 2021, **28**, 22.

41 R. Esquer and J. J. García, *J. Organomet. Chem.*, 2019, **902**, 120972.

42 Y. Wang, H. Song, H. Ge, J. Wang, Y. Wang, S. Jia, T. Deng and X. Hou, *J. Cleaner Prod.*, 2018, **176**, 873–879.

43 J. Stewart, M. Fuchs, J. Payne, O. Driscoll, G. Kociok-Kohn, B. D. Ward, S. Herres-Pawlis and M. D. Jones, *RSC Adv.*, 2022, **12**, 1416–1424.

44 S. D'Aniello, S. Laviéville, F. Santulli, M. Simon, M. Sellitto, C. Tedesco, C. M. Thomas and M. Mazzeo, *Catal. Sci. Technol.*, 2022, **12**, 6142–6154.

45 R. Lopez-Fonseca, I. Duque-Ingunza, B. de Rivasa, S. Arnaiz and J. I. Gutierrez-Ortiz, *Polym. Degrad. Stab.*, 2010, **95**, 1022–1028.

46 L. M. dos Santos, C. L. P. Carone, J. Dullius, R. Ligabue and S. Einloft, *Polímeros*, 2013, **23**(5), 608–613.

47 C. Molero, A. de Lucas and J. F. Rodriguez, *Polym. Degrad. Stab.*, 2009, **94**, 533–539.

48 J. T. Du, Q. Sun, X. F. Zeng, D. Wang, J. X. Wang and J. F. Chen, *Chem. Eng. Sci.*, 2020, **220**, 115642.
49 E. Selvam, Y. Luo, M. Ierapetritou, R. F. Lobo and D. G. Vlachos, *Catal. Today*, 2023, **418**, 114124.
50 J. Cao, Y. Lin, W. Jiang, W. Wang, X. Li, T. Zhou, P. Sun, B. Pan, A. Li and Q. Zhang, *ACS Sustain. Chem. Eng.*, 2022, **10**, 5476–5488.
51 M. Imran, D. H Kim, W. A. Al-Masry, A. Mahmooda, A. Hassan, S. Haider and S. M. Ramay, *Polym. Degrad. Stab.*, 2013, **98**, 904–915.
52 Y. Yang, F. Chen, T. Shen, A. Pariatamby, X. Wen, M. Yan and E. Kanchanatip, *Process Saf. Environ. Prot.*, 2023, **173**, 881–892.
53 M. Yan, Y. Yang, F. Chen, D. Hantoko, A. Pariatamby and E. Kanchanatip, *Environ. Sci. Pollut. Res.*, 2023, **30**, 102560–102573.
54 X. K. Li, H. Lu, W. Z. Guo, G. P. Cao, H. L. Liu and Y. H. Shi, *AIChE J.*, 2015, **61**, 200–214.
55 Q. Sun, Y. Y. Zheng, L. X. Yun, H. Wu, R. K. Liu, J. T. Du, Y. H. Gu, Z. G. Shen and J. X. Wang, *ACS Sustain. Chem. Eng.*, 2023, **11**, 7586–7595.
56 L. X. Yun, H. Wu, Z. G. Shen, J. W. Fu and J. X. Wang, *ACS Sustain. Chem. Eng.*, 2022, **10**, 5278–5287.
57 G. Eshaq and A. E. ElMetwally, *J. Mol. Liq.*, 2016, **214**, 1–6.
58 Y. D. Morcillo-Bolanos, W. J. Malule-Herrera, J. C. Ortiz-Arango and A. L. Villa-Holguin, *Rev. Fac. Ing. Univ. Antioq.*, 2018, **87**, 77–85.
59 S. G. Son, S. B. Jin, S. J. Kim, H. J. Park, J. Shin, T. Ryu, J. M. Jeong and B. G. Choi, *FlatChem*, 2022, **36**, 100430.
60 H. Yao, L. Liu, D. Yan, Q. Zhou, J. Xin, X. Lu and S. Zhang, *Chem. Eng. Sci.*, 2022, **248**, 117109.
61 R. X. Yang, Y. T. Bieh, C. H. Chen, C. Y. Hsu, Y. Kato, H. Yamamoto, C. K. Tsung and K. C. W. Wu, *ACS Sustain. Chem. Eng.*, 2021, **9**, 6541–6550.
62 (*a*) V. Tournier, C. M. Topham, A. Gilles, B. David, C. Folgoas, E. Moya-Leclair, E. Kamionka, M. L. Desrousseaux, H. Texier, S. Gavalda, M. Cot, E. Guemard, M. Dalibey, J. Nomme, G. Cioci, S. Barbe, M. Chateau, I. Andre, S. Duquesne and A. Marty, *Nature*, 2020, **580**, 216–219; (*b*) **https://www.carbios**.
63 B. Guo, X. Lopez-Lorenzo, Y. Fang, E. Backstrom, A. J. Capezza, S. R. Vanga, I. Furo, M. Hakkarainen and P. Syren, *ChemSusChem*, 2023, **16**, e202300742.
64 R. Xue, C. Qiu, X. Zhou, Y. Cheng, Z. Zhang, Y. Zhang, U. Schroder, U. T. Bornscheuer, W. Dong, R. Wei and M. Jiang, *Angew. Chem., Int. Ed.*, 2023, e202313633.
65 (*a*) L. Aer, Q. Jiang, I. Gul, Z. Qi, J. Feng and L. Tang, *Environ. Res.*, 2022, **212**, 113472; (*b*) M. E. Sevilla, M. D. Garcia, Y. Perez-Castillo, V. Armijos-Jaramillo, S. Casado, K. Vizuete, A. Debut and L. Cerda-Mejía, *Polymers*, 2023, **15**, 1779.
66 Y. Fang, K. Chao, J. He, Z. Wang and Z. Chen, *3 Biotech.*, 2023, **13**, 138.
67 F. Quartinello, S. Vajnhandl, J. Volmajer Valh, T. J. Farmer, B. Voncina, A. Lobnik, E. Herrero Acero, A. Pellis and G. M. Guebitz, *Microb. Biotechnol.*, 2017, **10**, 1376–1383.
68 A. Magnin, L. Entzmann, E. Pollet and L. Averous, *Waste Manag.*, 2021, **132**, 23–30.
69 F. Di Bisceglie, F. Quartinello, R. Vielnascher, G. M. Guebitz and A. Pellis, *Polymers*, 2022, **14**, 411.
70 J. Schmidt, R. Wei, T. Oeser, L. A. D. E. Silva, D. Breite, A. Schulze and W. Zimmermann, *Polymers*, 2017, **9**, 65.
71 R. Gautam, A. S. Bassi and E. K. Yanful, *Biotechnol. Lett.*, 2007, **29**, 1081–1825.
72 Y. Branson, S. Soltl, C. Buchmann, R. Wei, L. Schaffert, C. P. S. Badenhorst, L. Reisky, G. Jager and U. T. Bornscheuer, *Angew. Chem.*, 2023, **62**, e202216220.
73 D. De Smet, J. Verjans and M. Vanneste, *Polymers*, 2022, **14**, 5452.
74 J. Del Amo, D. Simon, M. J. Ramos, J. F. Rodriguez, A. De Lucas and A. M. Borreguero, *J. Mater. Cycles Waste Manage.*, 2022, **24**, 1059–1071.
75 D. Simon, A. M. Borreguero, A. De Lucas and J. F. Rodriguez, *Waste Manag.*, 2018, **76**, 147–171.
76 J. del Amo, A. M. Borreguero, M. J. Ramos and J. F. Rodriguez, *Polymers*, 2021, **13**, 1418.
77 R. Donadini, C. Boaretti, L. Scopel, A. Lorenzetti and M. Modesti, *Chem.–Eur. J.*, 2023, **30**, e202301919.
78 C. Molero, A. de Lucas, F. Romero and J. F. Rodriguez, *J. Mater. Cycles Waste Manage.*, 2009, **11**, 130–132.
79 M. Murai, M. Sanou, T. Fujimoto and F. Baba, *J. Cell. Plast.*, 2003, **39**, 15–27.
80 X. Gu, X. Wang, T. Wang, Y. Zhu, X. Guo, S. Liu, S. Zhu and Y. Liu, *Polymers*, 2022, **14**, 5450.
81 X. Luo and Y. Li, *J. Polym. Environ.*, 2014, **22**, 318–328.
82 Y. Lin, D. Yang, C. Meng, C. Si, Q. Zhang, G. Zeng and W. Jiang, *ChemSusChem*, 2023, **16**, e202300154.
83 C. Jeong, M. J. Hyun and Y. W. Suh, *Catal. Commun.*, 2015, **70**, 34–39.
84 W. Qingyin, K. Wukui, Z. Yi, Y. Xiangui, Y. Jie, C. Tong and W. Gongying, *Chin. J. Catal.*, 2013, **34**, 548–558.
85 W. Z. Guo, H. Lu, X. K. Li and G. P. Cao, *RSC Adv.*, 2016, **6**, 43171–43184.
86 S. Mohammadi and M. Enayati, *Polym. Degrad. Stab.*, 2022, **206**, 110180.
87 P. Uriz, M. Serra, P. Salagre, S. Castillon, C. Claver and E. Fernandez, *Tetrahedron Lett.*, 2002, **43**, 1673–1676.
88 (*a*) S. B. Jin, J. M. Jeong, S. G. Son, S. H. Park, K. G. Lee and B. G. Choi, *Mater. Today Commun.*, 2021, **26**, 101857; (*b*) G. Park, L. Bartolome, K. G. Lee, S. J. Lee, D. H. Kim and T. J. Park, *Nanoscale*, 2012, **4**, 3879–3885.
89 J. M. Jeong, S. B. Jin, S. G. Son, H. Suh, J. M. Moon and B. G. Choi, *React. Chem. Eng.*, 2021, **6**, 297–303.
90 M. Ammar, Y. Cao, P. He, L. Wang, J. Chen and H. Li, *Chin. J. Chem. Eng.*, 2017, **25**, 1760–1770.
91 Y. Cao, Y. Chi, A. Muhammad, P. He, L. Wang and H. Li, *Chin. J. Chem. Eng.*, 2019, **27**, 549–555.
92 B. Guo, J. Liu, S. Tang, Y. Liu, Z. Tiana and J. Lva, *J. Chem. Technol. Biotechnol.*, 2022, **97**, 1695–1704.
93 R. Wang, T. Wang, G. Yu and X. Chen, *Polym. Degrad. Stab.*, 2021, **183**, 109463.
94 M. E. E. Temporiti, L. Nicola, E. Nielsen and S. Tosi, *Microorganisms*, 2022, **10**, 1180.

95 R. P. Magalhaes, J. M. Cunha and S. F. Sousa, *Int. J. Mol. Sci.*, 2021, **22**, 11257.
96 S. Thiyagarajan, E. Maaskant-Reilink, T. A. Ewing, M. K. Julsing and J. van Haveren, *RSC Adv.*, 2022, **12**, 947–970.
97 A. Loredo-Trevino, G. Gutierrez-Sanchez, R. Rodriguez-Herrera and C. N. Aguilar, *J. Polym. Environ.*, 2012, **20**, 258–265.
98 (*a*) V. Petry do Canto, C. E. Thompson and P. A. Netz, *J. Mol. Graphics Modell.*, 2019, **89**, 82–95; (*b*) N. Mahajan and P. Gupta, *RSC Adv.*, 2015, **5**, 41839–41854; (*c*) M. Cregut, M. Bedas, M. J. Durand and G. Thouand, *Biotechnol. Adv.*, 2013, **31**, 1634–1647.
99 T. Nakajima-Kambe, Y. Shigeno-Akutsu, N. Nomura, F. Onuma and T. Nakahara, *Appl. Microbiol. Biotechnol.*, 1999, **51**, 134–140.
100 S. K. Phua, E. Castillo, J. M. Anderson and A. Hiltner, *J. Biomed. Mater. Res.*, 1987, **21**, 231–246.
101 G. Lin, S. Y. Chiou, B. C. Hwu and C. W. Hsieh, *Protein J.*, 2006, **25**, 33–43.
102 R. Salas, R. Villa, S. Cano, S. Nieto, E. Garcia-Verdugo and P. Lozano, *Catal. Today*, 2024, **430**, 114516.
103 R. Wei and W. Zimmermann, *J. Microb. Biotechnol.*, 2017, **10**, 1308–1322.
104 J. Ru, Y. Huo and Y. Yang, *Front. Microbiol.*, 2020, **11**, 442.
105 N. Mohanan, Z. Montazer, P. K. Sharma and D. B. Levin, *Front. Microbiol.*, 2020, **11**, 580709.
106 T. Su, T. Zhang, P. Liu, J. Bian, Y. Zheng, Y. Yuan, Q. Li, Q. Liang and Q. Qi, *Environ. Biotechnol.*, 2023, **107**, 1983–1995.
107 M. Giyahchi and H. Moghimi, *Nature*, 2023, **13**, 5016.
108 A. Magnin, E. Pollet, V. Phalip and L. Averous, *Biotechnol. Adv.*, 2020, **39**, 107457.
109 (*a*) V. Y. Suprun, V. I. Marukha and V. P. Sylovaniuk, *Mater. Sci.*, 2022, **57**, 755–764; (*b*) G. Rossignolo, G. Malucelli and A. Lorenzetti, *Green Chem.*, 2024, **26**, 1132–1152.
110 **https://www.repsol.com/en/sustainability/sustainability-pillars/environment/circular-economy/our-projects/chemical-recycling-of-polyurethane-foam/index.cshtml**.
111 **https://corporate.dow.com/en-us/purpose-in-action/circular-economy/renuva-program.html**.
112 **https://ioniqa.com/company/**.
113 **https://www.loopindustries.com/en**.
114 **https://www.indoramaventures.com/en/home**.
115 **https://www.carbios.com/fr/enzymatic-recycling/**.